

A modular framework for the development of targeted Covid-19 blood transcript profiling panels

Darawan Rinchai

Sidra Medicine, Doha, Qatar

Basirudeen Kabeer

Sidra Medicine, Doha, Qatar

Mohammed Toufiq

Sidra Medicine, Doha, Qatar

Zohreh Tatari-Calderone

Sidra Medicine, Doha, Qatar

Sara Deola

Sidra Medicine, Doha, Qatar

Tobias Brummaier

Shoklo Malaria Research Unit, Mahidol-Oxford Tropical Medicine Research Unit, Faculty of Tropical Medicine, Mahidol University, Mae Sot, Thailand

Mathieu Garand

Sidra Medicine, Doha, Qatar

Ricardo Branco

Sidra Medicine, Doha, Qatar

Nicole Baldwin

Baylor Institute for Immunology Research and Baylor Research Institute, Dallas, Texas, USA

Mohamed Alfaki

Sidra Medicine, Doha, Qatar

Matthew Altman

Division of Allergy and Infectious Diseases, University of Washington, Seattle, Washington, USA
Systems Immunology, Benaroya Research Institute, Seattle, Washington, USA

Alberto Ballestrero

Department of Internal Medicine, Università degli Studi di Genova, Genoa IT; IRCCS Ospedale Policlinico San Martino, Genoa IT

Matteo Bassetti

Division of Infectious and Tropical Diseases, IRCCS Ospedale Policlinico San Martino, Genoa, Italy;
Department of Health Sciences, University of Genoa, Italy

Gabriele Zoppoli

Department of Internal Medicine, Università degli Studi di Genova, Genoa IT; IRCCS Ospedale Policlinico San Martino, Genoa IT

Andrea De Maria

Division of Infectious and Tropical Diseases, IRCCS Ospedale Policlinico San Martino, Genoa, Italy;
Department of Health Sciences, University of Genoa, Italy

Benjamin Tang

Nepean Clinical School, University of Sydney, Sydney, NSW, Australia

Davide Bedognetti

Sidra Medicine, Doha, Qatar

Damien Chaussabel (✉ dchaussabel@sidra.org)

Sidra Medical and Research Center <https://orcid.org/0000-0002-6131-7242>

Research

Keywords: Blood transcriptomics, SARS-CoV-2, Covid-19, Immune monitoring

Posted Date: June 7th, 2020

DOI: <https://doi.org/10.21203/rs.3.rs-33274/v1>

License: © ⓘ This work is licensed under a Creative Commons Attribution 4.0 International License.

[Read Full License](#)

Version of Record: A version of this preprint was published on July 31st, 2020. See the published version at <https://doi.org/10.1186/s12967-020-02456-z>.

TITLE: A modular framework for the development of targeted Covid-19 blood transcript profiling panels

Darawan Rinchai^{1#}, Basirudeen Kabeer^{1#}, Mohammed Toufiq^{1#}, Zohreh Tatari-Calderone¹, Sara Deola¹, Tobias Brummaier^{2,3,4,5}, Mathieu Garand¹, Ricardo Branco¹, Nicole Baldwin⁶, Mohamed Alfaki¹, Matthew Altman^{7,8}, Alberto Ballestrero^{9,10}, Matteo Bassetti^{11,12}, Gabriele Zoppoli^{9,10}, Andrea De Maria^{11,12}, Benjamin Tang¹³, Davide Bedognetti¹ and Damien Chaussabel^{1*}

1 Sidra Medicine, Doha, Qatar

2 Shoklo Malaria Research Unit, Mahidol-Oxford Tropical Medicine Research Unit, Faculty of Tropical Medicine, Mahidol University, Mae Sot, Thailand

3 Centre for Tropical Medicine and Global Health, Nuffield Department of Medicine, University of Oxford, Oxford, United Kingdom

4 Swiss Tropical and Public Health Institute, Basel, Switzerland

5 University of Basel, Basel, Switzerland

6 Baylor Institute for Immunology Research and Baylor Research Institute, Dallas, Texas, USA

7 Division of Allergy and Infectious Diseases, University of Washington, Seattle, Washington, USA

8 Systems Immunology, Benaroya Research Institute, Seattle, Washington, USA

9 Department of Internal Medicine, Università degli Studi di Genova, Genoa IT

10 IRCCS Ospedale Policlinico San Martino, Genoa IT

11 Division of Infectious and Tropical Diseases, IRCCS Ospedale Policlinico San Martino, Genoa, Italy

12 Department of Health Sciences, University of Genoa, Italy

13 Nepean Clinical School, University of Sydney, Sydney, NSW, Australia

Equal contributing authors

*To whom correspondence may be addressed

dchaussabel@sidra.org

1 **ABSTRACT**

2 **Background:** Covid-19 morbidity and mortality are associated with a dysregulated immune
3 response. Tools are needed to enhance existing immune profiling capabilities in affected
4 patients. Here we aimed to develop an approach to support the design of focused blood
5 transcriptome panels for profiling the immune response to SARS-CoV-2 infection.

6 **Methods:** We designed a pool of candidates based on a pre-existing and well-characterized
7 repertoire of blood transcriptional modules. Available Covid-19 blood transcriptome data was
8 also used to guide this process. Further selection steps relied on expert curation.
9 Additionally, we developed several custom web applications to support the evaluation of
10 candidates.

11 **Results:** As a proof of principle, we designed three targeted blood transcript panels, each
12 with a different translational connotation: immunological relevance, therapeutic development
13 relevance and SARS biology relevance.

14 **Conclusion:** Altogether the work presented here may contribute to the future expansion of
15 immune profiling capabilities via targeted profiling of blood transcript abundance in Covid-19
16 patients.

17

18

19

20

21

22

23

24

25

26 **Keywords:** Blood transcriptomics, SARS-CoV-2, Covid-19, Immune monitoring

27 **BACKGROUND**

28 Covid-19 is an infectious, respiratory disease caused by a newly discovered coronavirus:
29 SARS-CoV-2. The severity of symptoms and the course of infection vary widely, with most
30 patients presenting mild symptoms. However, about 20% of patients develop severe disease
31 and require hospitalization (1,2). The interaction between innate and adaptive immunity can
32 lead to the development of neutralizing antibodies against SARS-CoV-2 antigens that might
33 be associated with viral clearance and protection (3). But immune factors are also believed
34 to play an important role in the rapid clinical deterioration observed in some Covid-19
35 patients (4). There is thus a need to develop new modalities that can improve the delineation
36 of “immune trajectories” during SARS-CoV-2 infection.

37 Blood transcriptome profiling involves measuring the abundance of circulating
38 leukocyte RNA on a genome-wide scale via RNA sequencing (5). Processing of the samples
39 and the raw sequencing data however, is time consuming and requires access to
40 sophisticated laboratory and computational infrastructure. Thus, the possibility of
41 implementing this approach on large scales to ensure immediate translational potential is
42 limited. Such unbiased omics profiling data might rather be leveraged to inform the
43 development of more practical, scalable and targeted transcriptional profiling assays. These
44 assays could in turn serve to significantly bolster existing immune profiling capacity.

45 Fixed sets of transcripts grouped based on co-expression observed in large
46 collections of reference datasets provide a robust platform for transcriptional profiling data
47 analyses (6). Here we leveraged a repertoire of 382 transcriptional modules previously
48 developed by our team (7). The repertoire is based on a collection of reference patient
49 cohorts encompassing 16 pathological or physiological states and 985 individual
50 transcriptome profiles. In this proof of principle study, we used the available transcript
51 profiling data from two separate studies to select Covid-19 relevant sets of modules (8,9).
52 Next, we applied filters based on pre-specified selection criteria (e.g. immunologic relevance
53 or therapeutic relevance). Finally, expert curation was used as the last selection step. For
54 this we have developed custom web applications to consolidate the information necessary

55 for the evaluation of candidates. One of these applications provides access to module-level
56 transcript abundance profiles for available Covid-19 blood transcriptome profiling datasets.
57 Another web interface was implemented which serves as a scaffold for the juxtaposition of
58 such transcriptional profiling data with extensive functional annotations.

59

60 **METHODS**

61 **Datasets**

62 Two Covid-19 blood transcriptional datasets available at the time this work was conducted
63 were used: **1)** Xiong *et al.* (9) obtained peripheral mononuclear cell samples obtained from
64 one uninfected control individual and three patients with Covid-19. RNA abundance was
65 profiled via RNAseq. The data were deposited in the Genome Sequence Archive of the
66 Beijing Institute of Genomics, Chinese Academy of Sciences, under the accession number
67 CRA002390. FASTQ passed QC and were aligned to reference genome GRChg38/hg19
68 using Hisat2 (v2.05). BAM files were converted to a raw count expression matrix using
69 subreads (v1.6.2). Raw expression data was corrected for within lane and between lane
70 effects using R package EDASeq (v2.12.0) and quantile normalized using preprocessCore
71 (v1.36.0). The modular analysis was performed by using 10,617 RNA-seq genes which
72 overlapped with transcripts from the 3rd generation module construction (7). details of the
73 analysis as described below section.

74 **2)** Ong *et al.* (8) collected whole blood stabilized in RNA buffer from uninfected
75 controls and three Covid-19 patients at multiple time points. RNA abundance was profiled
76 using a standard immunology panel from Nanostring comprising 594 transcripts. The data
77 were deposited in the arrayexpress public repository with accession ID E-MTAB-8871. The
78 normalized data were downloaded, and modular analysis was performed by using 403
79 NanoString genes which overlapped with transcripts from the 3rd generation module
80 construction details of the analysis as described below section.

81 **3)** We also used a reference dataset generated by our group that was previously
82 used to construct the 382 blood transcriptional module repertoire (7). Briefly, this repertoire

83 consists of the following cohorts of patients and respective control subjects: *S. aureus*
84 infection (99 cases, 44 controls), sepsis (35 cases, 12 controls), tuberculosis (23 cases, 11
85 controls), Influenza (25 cases, 14 controls), RSV infection (70 cases, 14 controls), HIV
86 infection (28 cases, 35 controls), systemic lupus erythematosus (55 cases, 14 controls),
87 multiple sclerosis (34 cases, 22 controls), juvenile dermatomyositis (40 cases, 9 controls),
88 Kawasaki disease (21 cases, 23 controls), systemic onset idiopathic arthritis (62 cases, 23
89 controls), COPD (19 cases, 24 controls), melanoma (22 cases, 5 controls), pregnancy (25
90 cases, 20 controls), liver transplant recipients (94 cases, 30 controls), and B-cell deficiency
91 (20 cases, 13 controls). All samples were run at the same facility on Illumina HumanHT-12
92 v3.0 Gene Expression BeadChips. The data have been deposited in NCBI Gene Expression
93 Omnibus (GEO) with accession number GSE100150.

94

95 **Transcriptional module repertoire**

96 The method used to construct the transcriptional module repertoire has been described
97 elsewhere (10,11). The version used here is the third and last to have been developed by
98 our group over a period of 12 years. It is the object of a separate publication (available on a
99 pre-print server (7)).

100 Briefly, the approach consists of identifying sets of co-expressed transcripts in a wide
101 range of pathological or physiological states, focusing in this case on the blood
102 transcriptome as the biological system. We determined co-expression based on patterns of
103 co-clustering observed for all gene pairs across the collection of 16 reference datasets listed
104 in the previous section and that encompassed viral and bacterial infectious diseases as well
105 as several inflammatory or autoimmune diseases, B-cell deficiency, liver transplantation,
106 stage IV melanoma and pregnancy. Overall, this collection comprised 985 blood
107 transcriptome profiles. A weighted, co-expression network was built with the weight of the
108 nodes connecting a gene pair being based on the number of times co-clustering was
109 observed for the pair among the 16 reference datasets. Thus, the weights ranged from 1
110 (where co-clustering occurs in one of 16 datasets) to 16 (where co-clustering occurs in all 16

111 datasets). Next, this network was mined using a graph theory algorithm to define subsets of
112 densely connected gene sets that constituted our module repertoire (“Cliques” and
113 “Paracliques”).

114 Overall, 382 transcriptional modules were identified, encompassing 14,168
115 transcripts. A supplemental file including the definition of this module repertoire along with
116 the functional annotations is available elsewhere (7). To provide another level of granularity
117 and facilitate data interpretation, a second round of clustering was performed to group the
118 modules into “aggregates”. This process was achieved by grouping the set of 382 modules
119 according to the patterns of transcript abundance across the 16 reference datasets that were
120 used for module construction. This segregation resulted in the formation of 38 aggregates,
121 each comprising between one and 42 modules.

122

123 **Module repertoire analyses**

124 The modular analyses were performed using the core set of 14,168 transcripts forming the
125 module repertoire. For group-level comparisons (cases vs controls), a paired t-test was
126 performed on the log₂-transformed data [Fold change (FC) cut off = 1.5; FDR cut off = 0.1].
127 For individual-level analyses, each sample was compared to the mean value of the
128 corresponding control samples (or individual sample in the case of the Xiong *et al.* dataset).
129 The cut off comprised an absolute FC >1.5 and a difference in counts >10. The results for
130 each module are reported as the percentage of its constitutive transcripts that increased or
131 decreased in abundance. Because the genes comprised in a module are selected based on
132 the co-expression observed in blood, the changes in abundance within a given module tend
133 to be coordinated and the dominant trend is therefore selected (the greater value of the
134 percentage increased vs. percentage decreased). Thus, the values range from -100% (all
135 constitutive modules are decreased) to +100% (all constitutive modules are increased). A
136 module was considered to be “responsive” when the proportion of transcripts found to be
137 increased was >15% (induced), or when the proportion of transcripts found to be decreased

138 was $\leq 15\%$ (repressed). At the aggregate-level, the percent values of the constitutive
139 modules were averaged.

140

141 **Data visualization**

142 Changes in transcript abundance reduced at the module or module aggregate-level were
143 visualized using a custom fingerprint heatmap format. For each module, the percentage of
144 increased transcripts is represented by a red spot and the percentage of decreased
145 transcripts is represented by a blue spot. The fingerprint grid plots were generated using
146 “ComplexHeatmap” (12). A web application was developed to generate the plots and browse
147 modules and module aggregates (https://drinchai.shinyapps.io/COVID_19_project/). A
148 detailed description and source code will be available as part of a separate publication
149 BioRxiv deposition on GitHub and BioRxiv (in preparation).

150

151 **Selection of transcripts for inclusion in targeted panels**

152 Therapeutic relevance: Covid-19 module sets belonging to aggregates comprising module
153 annotations relating to inflammation, monocytes, neutrophils or coagulation pathway were
154 selected for screening (A7, A8, A26, A31, A33, A34, A35). In turn, transcripts from each of
155 the corresponding module sets were selected on the basis of their status as a known
156 therapeutic target of a drug for which clinical precedence exists (source:
157 targetvalidation.org). Next, candidates were prioritized via expert curation on the basis of
158 compatibility and a potential benefit as a Covid-19 treatment. Curators were tasked with
159 prioritizing candidates within each of the Covid-19 module sets. Only the top ranked
160 candidate from each set was selected for inclusion in the panel. Module sets from aggregate
161 A28 (interferon response) may also be of clinical relevance, may also be of clinical
162 relevance, as indicators of a treatment response since interferon administration has been
163 shown to increase the activity of anti-viral drugs in Covid-19 patients (13). The selection of
164 candidates for aggregate A28 sets was thus based on the amplitude of the response to beta-
165 interferon therapy measured in patients with multiple sclerosis [fold-change over pre-

166 treatment baseline (14) & NCBI GEO accession GSE26104]. The remaining nine
167 aggregates, which tended to associate preferentially with adaptive immune responses and
168 for which targeting by therapies might prove detrimental, were not included in this screen.
169 For these, representative transcripts from the default panel of immune relevant transcripts
170 were included.

171 Relevance to Coronavirus biology: for the second panel, transcripts were primarily selected
172 based on their relevance to SARS (Severe Acute Respiratory Syndrome) biology. As a first
173 step, a literature profiling tool was used to identify among the SARS, MERS (Middle East
174 Respiratory Syndrome), or Covid-19 literature articles that were associated with transcripts
175 forming the 28 Covid-19 module sets [Literature Lab (LitLab) by Acumenta Biotech (15) and
176 LitLab Gene Retriever application, Accumenta Biotech, Boston, MA]. Next, the potential
177 associations were assessed by manual curation. The curators prioritized the transcripts for
178 which the associations could be confirmed based on importance and robustness.

179 Immunological relevance: Lists of immunologically relevant genes were retrieved
180 from Immport (16), and were used along with membership to IPA pathways (Ingenuity
181 Pathway Analysis, QIAGEN, Germantown MD) to annotate transcripts comprising Covid-19
182 module sets. The curators prioritized annotated transcripts on the basis of their relevance to
183 the functional annotations of the module set (e.g. interferon, inflammation, cytotoxic cells).
184 The transcript with the highest priority rank was included in the assay.

185 Housekeeping genes: A recommended set of housekeeping genes is provided in
186 **Table 6**. These were selected on the basis of low variance observed across the 985
187 transcriptome profiles generated for our reference cohorts.

188

189 **Annotation framework**

190 Links to the resources described in this section and to video demonstrations are available in
191 **Table 2**. Interactive presentations were created via the Prezi web application. For this we
192 have built and expanded upon an annotation framework established as part of the
193 characterization of our reference blood transcriptome repertoire (7). Several bioinformatic

194 resources were used to populate interactive presentations that served as a framework for
195 annotation of Covid-19 relevant module sets. These resources include web applications
196 deployed using Shiny R, which permit to plot transcript abundance patterns at the module
197 and aggregate levels. Two of these applications were developed as part of a previous work
198 establishing the blood transcriptome repertoire and applying it in the context of a meta-
199 analysis of six public RSV datasets (17). A third application was developed as part of this
200 work and can generate profiles at the transcript, module and module-aggregate levels for the
201 Xiong *et al.* and Ong *et al.* datasets.

202

203 **RESULTS**

204

205 **Mapping Covid-19 blood transcriptome signatures against a pre-existing reference set** 206 **of transcriptional modules**

207 SARS-CoV-2 infection might not result in changes in transcript abundance across all of the
208 382 transcriptional modules constituting our repertoire [(comprising 14,168 transcripts) see
209 methods section and (7)]. Indeed, the 16 reference patient cohorts upon which our repertoire
210 was based encompass a wide range of immune states, including infectious diseases but
211 also autoimmune diseases, pregnancy and cancer. Thus, the first step involved identifying
212 subsets of modules for which changes could be observed in Covid-19 patients.

213 We used two sets of Covid-19 patients for this proof of principle analysis. These
214 datasets were contributed by Xiong *et al.* (9) (one control and three subjects) and Ong *et al.*
215 (8) (nine controls and three subjects profiled at multiple time points). Their data were
216 generated using RNA-seq and Nanostring technology, respectively. The generic 594
217 transcript panel used by Ong *et al.* did not give sufficient coverage across the 382-module
218 set. We thus mapped the transcript changes at a lower resolution, using a framework formed
219 by 38 module “aggregates“. These 38 aggregates were constituted by grouping modules
220 based on similarities in abundance patterns across the 16 reference datasets [see methods
221 section and (7)].

222 We first assessed changes in transcript abundance resulting from SARS-CoV-2
223 infection across the 38 module aggregates (**Figure 1**). In general, we saw a decrease in
224 aggregates associated with lymphocytic compartments (aggregates A1 & A5) and an
225 increase in aggregates associated with myeloid compartments and inflammation
226 (aggregates A33 & A35). As expected, we also saw increases over uninfected controls for
227 the module aggregate associated with interferon (IFN) responses (A28) and the module
228 aggregate presumably associated with the effector humoral response (A27). We detected a
229 wide spread of values for aggregate A11 for the Nanostring (Ong *et al.*) dataset. However,
230 this aggregate comprises only one module, with only two of its transcripts measured in this
231 Nanostring code set (the probe coverage across all aggregates is shown in **Supplementary**
232 **Figure 1**).

233 Despite large differences between the two studies in terms of design, range of
234 clinical severity, technology platforms and module coverage, the combined overall changes
235 (detected at a high-level perspective) are consistent with those observed in known acute
236 infections, such as those caused by influenza, respiratory syncytial virus (RSV) or *S. aureus*.
237 This consistency is evidenced by the patterns of change observed for the reference
238 fingerprints shown alongside those of Covid-19 patients (**Figure 1**).

239 Overall, such a high-level analysis allows us to identify module aggregates forming
240 our repertoire that may be included in further selection steps. In this proof of principle
241 analysis, we selected 17 aggregates for further analysis (**Table 1**).

242

243 **Identification of coherent sets of Covid-19-relevant modules**

244 The abundance patterns for modules comprised in a given aggregate are not always
245 homogeneous (**Figure 2**). Thus, a next step would consist of identifying sets of modules
246 within an aggregate that display coherent abundance patterns across modules forming a
247 given aggregate.

248 To achieve this, we first mapped the changes in transcript abundance associated
249 with Covid-19 disease using the RNAseq dataset from Xiong *et al.*, as illustrated for A31

250 (Figure 2A) and A28 (Figure 3A). Similar plots can be generated for all other aggregates
251 using the “COVID-19” web application (also compiled in **Supplementary File 1** and listed in
252 **Table 2**). Next, we identified and assigned a module set ID for each the modules that formed
253 homogeneous clusters. For example, we designated the first A28 set as A28/S1. Such
254 module grouping is only based on patterns of transcript abundance observed in three Covid-
255 19 patients; however, the groupings were often consistent with those observed for the much
256 larger reference cohorts that constitute the module repertoire (**Figure 2B** and **Figure 3B**).
257 A28/S1, which is formed by M8.3 and M15.127, serves as a good example of this
258 consistency (**Figure 3B**). Likewise, the segregation of the modules forming A31 based on
259 differences observed in the three Covid-19 patients was also apparent in the reference
260 patient cohorts (**Figure 2B**). Specifically, an increase in A31/S1 modules, which
261 accompanied a decrease in A31/S2 modules, in these three patients was also characteristic
262 of RSV patients.

263 We ultimately derived 28 homogeneous Covid-19 relevant module sets from the 17
264 aggregates selected in the earlier step (**Table 1**). These sets might be used as a basis for
265 further selection.

266

267 **Design of an illustrative targeted panel emphasizing immunological relevance**

268 In the previous step, we used available Covid-19 data to guide the selection of 28 distinct
269 “Covid-19 relevant module sets”. In the next step, we selected the transcripts within each
270 module set that warranted inclusion in one of three illustrative Covid-19 targeted panels. A
271 first panel was formed using immunologic relevance as the primary criterion, a second was
272 formed on the basis of relevance to coronavirus biology, a third was constituted on the basis
273 of relevance to therapy.

274 For the first panel we matched transcripts comprised in each module set to a list of
275 canonical immune genes (see methods for details). Expert curation also involved accessing
276 transcript profiling data from the reference datasets, indicating for instance leukocyte
277 restriction or patterns of response to a wide range of immune stimuli *in vitro*. We describe

278 our approach for module and gene annotation in more detail below and provide access to
279 our resources to support expert curation (**Table 2**).

280 For our illustrative case, we selected one representative transcript per module set to
281 produce a panel comprised of 28 representative transcripts (**Table 3**). Examples of
282 signatures surveyed by such a panel include: **1) ISG15** in A28/S1 (interferon responses),
283 which encodes for a member of the ubiquitin family. ISG15 plays a central role in the host
284 defense to viral infections (18). **2) GATA1** in A37/S1 (erythroid cells), which encodes for a
285 master regulator of erythropoiesis (19). It is associated with a module signature (A37) that
286 we recently reported as being associated with immunosuppressive states, such as late stage
287 cancer and maintenance immunosuppressive therapy in solid organ transplant recipients
288 (17). In the same report we also found an association between this signature and
289 heightened severity in patients with RSV infection and established a putative link with a
290 population of immunosuppressive circulating erythroid cells (20). **3) CD38** in A27/S1 (cell
291 cycle), which encodes for the CD38 molecule expressed on different circulating leukocyte
292 populations. In whole blood we find the abundance of its transcript correlate with that of IGJ,
293 TNFRSF17 (BCMA), TXNDC5 (M12.15). Such a signature was previously found to be
294 increased in response to vaccination at day 7 post administration, to correlate with the
295 prevalence of antibody producing cells, and the development of antibody titers at day 28
296 (21). **4) TLR8** in A35/S1 (inflammation), encodes toll-like receptor 8. Expression of
297 transcripts comprising this aggregate is generally restricted to neutrophils and robustly
298 increased during sepsis (e.g. as we have described in detail earlier for ACSL1, another
299 transcript belonging to this aggregate (22)). **5) GZMB** in A2/S1 (Cytotoxic cells) encodes
300 Granzyme B, a serine protease known to play a role in immune-mediated cytotoxicity. Other
301 transcripts forming this panel are listed in **Table 3**.

302 Even with the limited amount of data available to guide the selection in the previous
303 steps, it is reasonable to assume that such a panel (while not optimal) would already provide
304 valid information for Covid-19 immune profiling. Additional Covid-19 blood transcriptome

305 data that will become available in the coming weeks will allow us to refine the overall
306 selection process.

307

308 **Design of an illustrative targeted panel emphasizing therapeutic relevance**

309 A different translational connotation was given for this second panel. Here, we based
310 the selection on the same collection of 28 module sets. However, this time, whenever
311 possible, we included transcripts that could have value as targets for the treatment of Covid-
312 19 patients. An initial screen identified 82 transcripts encoding molecules that are known
313 targets for existing drugs (see Methods). We further prioritized these candidates based on
314 an expert's evaluation of the compatibility of use of the drugs for treating Covid-19 patients.
315 As an exception, module sets belonging to A28 (interferon response) were selected based
316 on their suitability as markers of a response to interferon therapy. Sets for which no targets
317 of clinical relevance were identified (16/28) were instead represented in the panel by
318 immunologically-relevant transcripts (defined earlier).

319 We ultimately identified a preliminary set of 12 targets through this high stringency
320 selection process (**Table 4**). Developing effective immune modulation therapies in critical
321 care settings has proven challenging (23). Current efforts in the context of Covid-19 disease
322 particularly aim at controlling runaway systemic immune responses or so called "cytokine
323 storms" that have been associated with organ damage and clinical worsening. Targets of
324 interest identified among our gene set include: **1) IL6R** in A35/S2 (inflammation), encoding
325 the Interleukin-6 Receptor, which is a target for the biologic drug Tocilizumab. Several
326 studies have tested this antagonist in open label single arm trials in Covid-19 patients with
327 the intent of blocking the cytokine storm associated with severe Covid-19 infection (24,25).
328 **2) CCR2** in A26/1 (monocytes), encoding the chemokine (C-C motif) receptor 2, is targeted
329 along with CCR5 by the drug Cenicriviroc. This drug exerts potent anti-inflammatory activity
330 (26). **3) TBXA2R** in A31/1 (platelets), encoding the Thromboxane receptor, is targeted by
331 several drugs with anti-platelet aggregation properties (27). **4) PDE8A** in A33/S1
332 (inflammation), encoding Phosphodiesterase 8A, is targeted by Pentoxifylline, a non-

333 selective phosphodiesterase inhibitor that increases perfusion and may reduce risk of acute
334 kidney injury and attenuates LPS-induced inflammation (28). **5) NQO1** in A8/S1
335 (Complement), encoding NAD(P)H quinone dehydrogenase 1. The NQO1 antagonist
336 Vatiquinone (EPI-743) has been found to inhibit ferroptosis (29), a process associated with
337 tissue injury (30), including in sepsis (31). A complete list is provided in **Table 4**.

338 The fact that this transcript panel and the previous survey the same pre-defined 28
339 homogenous Covid-19 relevant module sets should make them largely synonymous (since
340 modules are formed on the basis of co-expression). Nevertheless, this second panel may be
341 more relevant for investigators interested in investigating new therapeutic approaches or
342 measuring responses to treatment.

343

344 **Design of a targeted panel of blood transcripts of relevance for SARS-CoV-2 biology**

345 For the third panel designed in this proof of principle, we primarily selected
346 transcripts based on their relevance to SARS biology. As a first step, we used a literature
347 profiling tool to identify SARS, MERS, or Covid-19 literature articles that were associated
348 with transcripts forming the 28 Covid-19 module sets. Next, the potential associations were
349 subjected to expert curation (see Methods). Once again, to keep redundancies to a
350 minimum, we only included one candidate per set in this panel (**Table 5**). Notable examples
351 include: **1) LTF** in A38/S1 (neutrophil activation) encodes Lactotransferrin, that is known to
352 block the binding of the SARS-CoV spike protein to host cells, thus exerting an inhibitory
353 function at the viral attachment stage (32). **2) FURIN** in A37/S1 (Erythroid cells), encodes a
354 proprotein convertase that preactivates SARS-CoV-2, thus reducing its dependence on
355 target cell proteases for entry (33). **3) EGR1** in A7/S1 (Monocytes), encodes Early Growth
356 Response 1, which upon induction by SARS Coronavirus Papain-Like Protease mediates
357 up-Regulation of TGF- β 1 (34). **4) STAT1** in A28/S3 (Interferon response), encodes a
358 transcription factor known to play an important role in the induction of antiviral effector
359 responses. It was reported that SARS ORF6 antagonizes STAT1 function by preventing its

360 translocation to the nucleus and acts as an interferon antagonist in the context of SARS-CoV
361 infection (35).

362 This screen identified several molecules that may be of importance for SARS-CoV-2
363 entry and replication. A complete list is provided in **Table 4**. It is expected that this
364 knowledge will evolve rapidly over time and frequent updates may be necessary. And, as for
365 the previous two panels, investigators may also have an interest in including more than one
366 candidate per module set. This of course would also be feasible, although at the expense of
367 course of parsimony.

368

369 **Development of an annotation framework in support of signatures curation efforts**

370 A vast amount of information is available to support the work of expert curators who are
371 responsible for finalizing the selection of candidates. This process often requires accessing
372 a number of different resources (e.g. those listed in **Table 2**). Here we have built upon
373 earlier efforts to aggregate this information in a manner that makes it seamlessly accessible
374 by the curators.

375 As proof of principle, we created dedicated, interactive presentations in Prezi for
376 module aggregates A28 (<https://prezi.com/view/7lbgGwfiNffqQzvL14/>) and A31
377 (<https://prezi.com/view/zYCSLyo0nvJTwjfJkJqb/>). These presentations are intended, on the
378 one hand, to aggregate contextual information that can serve as a basis for data
379 interpretation. On the other hand, they are intended to capture the results of the
380 interpretative efforts of expert curators.

381 The interactive presentations are organized in sections, each showing aggregated
382 information from a different level: module-sets, modules and transcripts (**Figure 5**). The
383 information derived from multiple online sources, including both third party applications and
384 custom applications developed by our team (**Table 2**). Among those is a web application
385 developed specifically for this work, which was used to generate the Covid-19 plots from
386 Ong *et al.* and Xiong *et al.* (**Figure 5A**). The interactive presentation itself permits to zoom in
387 and out, determine spatial relationships and interactively browse the very large compendium

388 of analysis reports and heatmaps generated as part of these annotation efforts. The last
389 section that contains transcript-centric information, is also the area where interpretations
390 from individual curators is aggregated.

391 We have annotated and interpreted some of the transcripts included in **A31/S1** in
392 such a manner: **1) OXTR**, which encodes for the Oxytocin receptor through which anti-
393 inflammatory and wound healing properties of Oxytocin are mediated (36). Among our
394 reference cohort datasets, OXTR is most highly increased in patients with *S. aureus*
395 infection or active pulmonary tuberculosis (7). **2) CD9**, which encodes a member of the
396 tetraspanin family, facilitates the condensation of receptors and proteases activating MERS-
397 CoV and promoting its rapid and efficient entry into host cells (37). **3) TNFSF4**, which
398 encodes for OX40L and is a member of the TNF superfamily. Although OX40L is best known
399 as a T-cell co-stimulatory molecule, reports have also shown that it is present on the
400 neutrophil surface (38). Furthermore, OX40L blockade improved outcomes of sepsis in an
401 animal model.

402 Our interpretation efforts have been limited thus far by expediency. Certainly,
403 interpretation will be the object of future, more targeted efforts. In the meantime, this
404 annotation framework supports the selection of candidates forming the panels presented
405 here. It may also serve as a resource for investigators who wish to design custom panels of
406 their own.

407

408 **DISCUSSION**

409 Early reports point to profound immunological changes occurring in affected patients during
410 the course of a SARS-CoV-2 infection (39,40). In particular, patterns of immune dysfunction
411 have been associated with clinical deterioration and the onset of severe respiratory failure
412 (41). However, disease outcomes remain highly heterogeneous and factors contributing to
413 clinical deterioration are poorly understood. Among other modalities, means to establish
414 comprehensive immune monitoring in cohorts of Covid-19 patients are needed.

415 Here we designed an approach to select and curate targeted blood transcript panels
416 relevant to Covid-19. When finalized, such panels could in turn serve as a basis for rapid
417 implementation of focused transcript profiling assays. This process should become possible
418 as more Covid-19 blood transcriptome profiling datasets become available in the coming
419 weeks and months. These data could, for instance, be used to refine the delineation of
420 Covid-19 module sets.

421 Because our selection strategy relies primarily on a pre-existing module repertoire
422 framework, we anticipate that changes would only be relatively minor. Indeed, one
423 advantage of basing candidate selection on a repertoire of transcriptional modules is that it
424 permits to derive non-synonymous transcripts sets. In other words, each transcript included
425 in the panel could survey the abundance of a different module (signature). Basing selection
426 on differential expression instead, for instance, would tend to select multiple transcripts from
427 more dominant signatures (with highest significance / fold changes). But for more specific
428 purposes, such as differential diagnosis or prediction, machine learning models would be
429 more appropriate [as demonstrated for instance in sepsis studies: (42)]. Indeed, such panels
430 have already been developed for Covid-19 (43), and we anticipate that more will emerge
431 over the coming months. However, our intent here was different: our primary aim was to
432 support the development of a solution that can monitor immune responses and functions.

433 Delineation of “immune trajectories” associated with clinical deterioration of Covid-19
434 patients is one application to consider. Another application would be the measurement of
435 responses to therapy (as part of standard of care or a trial). The immune profiling of
436 asymptomatic or pre-symptomatic patients (e.g. quarantined) would be another setting
437 where implementation of such an assay could prove useful. For this, it would for instance be
438 possible to use protocols that we have previously developed for home-based, self-sampling
439 and blood RNA stabilization (44,45).

440 Different connotations were given for the three panels, which are presented here as
441 a proof of principle. The panel consisting of immunologically relevant markers might have
442 the highest general interest. However, measuring changes in the abundance of transcripts

443 coding for molecules that are targetable by existing drugs could have higher translational
444 potential. Another illustrative panel comprises transcripts coding for molecules that are of
445 relevance to SARS-CoV-2 biology and might be of additional interest in investigations of
446 host–pathogens interactions. The common denominator between these panels is that they
447 comprise representative transcripts of each of the 28 module sets. Other transcript
448 combinations following the same principle would be possible, as well as the inclusion of
449 multiple transcripts from the same set for added robustness. The obvious disadvantage of
450 the latter, however, is the increase to the size of the panel. Medium-throughput technology
451 platforms, such as the Nanostring nCounter System, Fluidigm Biomark or ThermoFisher
452 Openarray, would be appropriate for implementing custom profiling assays with the number
453 of targets comprising the tentative panels presented here (or a combination thereof).
454 Downsizing panels to comprise ± 10 key markers might serve as a basis for implementation
455 on more ubiquitous real-time PCR platforms.

456

457 **CONCLUSIONS**

458 Overall, this work lays the ground for a framework that could support the
459 development of increasingly refined and interpretable targeted panels for profiling immune
460 responses to SARS-CoV-2 infection. This should be possible in part by providing curators
461 with seamless access to vast amounts of annotations aggregated from different sources.

462

463 **LIST OF ABBREVIATIONS**

464 SARS: Severe Acute Respiratory Syndrome; MERS: Middle East Respiratory Syndrome;
465 RSV: Respiratory Syncytial Virus; GEO: Gene Expression Omnibus

466

467 **DECLARATIONS**

468 ***Ethics approval and consent to participate***

469 Not applicable

470

471 **Consent for publication**

472 Not applicable

473

474 **Availability of data and materials**

475 *The datasets generated during and/or analysed during the current study are available:*

476 - *in the ArrayExpress repository, under the accession number E-MTAB-8871,*

477 <https://www.ebi.ac.uk/arrayexpress/experiments/E-MTAB-8871/>

478 - *in the Genome Sequence Archive of the Beijing Institute of Genomics, Chinese*

479 *Academy of Sciences, under the accession number CRA002390,*

480 <https://bigd.big.ac.cn/gsa/browse/CRA002390>

481 - *In the NCBI GEO database, under the accession numbers*

482 ○ *GSE26104, <https://www.ncbi.nlm.nih.gov/geo/query/acc.cgi?acc=GSE26104>*

483 ○ *GSE100150, <https://www.ncbi.nlm.nih.gov/geo/query/acc.cgi?acc=GSE100150>*

484

485 **Competing interests**

486 The authors declare that they have no competing interests.

487

488 **Funding**

489 Development of some of the bioinformatic resources and approaches employed here was

490 supported by NPRP grant # 10-0205-170348 from the Qatar National Research Fund (a

491 member of Qatar Foundation). The work reported herein is solely the responsibility of the

492 authors.

493

494 **Authors' contributions**

495 DR, BK, MT, NB, MAIt, MB, GZ, ADM, BT, DB, DC conceptualization. DR, BK, MT, ZC, SD,

496 TB, MG: data curation and validation. DR, BK, MT and DC: visualization. DR, BK, MT, ZC,

497 SD, TB, MG, DB, DC: analysis and interpretation. DB, DC: funding acquisition. DR and DC:

498 methodology development. DR, BK, MT, DC: writing of the first draft. DR, MT, MAIf: software

499 development and database maintenance. DR, BK, MT, ZC, SD, TB, MG, RB, NB, MAIf,
500 MAIt, AB, MB, GZ, ADM, BT, DB, DC writing–review and editing The contributor's roles listed
501 above follow the Contributor Roles Taxonomy (CRediT) managed by The Consortia
502 Advancing Standards in Research Administration Information (CASRAI)
503 (<https://casrai.org/credit/>).

504

505 **Acknowledgements**

506 Not applicable.

507

508 **REFERENCES**

- 509 1. Yang W, Cao Q, Qin L, Wang X, Cheng Z, Pan A, et al. Clinical characteristics and
510 imaging manifestations of the 2019 novel coronavirus disease (COVID-19):A multi-
511 center study in Wenzhou city, Zhejiang, China. *J Infect.* 2020;80(4):388–93.
- 512 2. Guan W-J, Ni Z-Y, Hu Y, Liang W-H, Ou C-Q, He J-X, et al. Clinical Characteristics of
513 Coronavirus Disease 2019 in China. *N Engl J Med.* 2020 30;382(18):1708–20.
- 514 3. Long Q-X, Liu B-Z, Deng H-J, Wu G-C, Deng K, Chen Y-K, et al. Antibody responses
515 to SARS-CoV-2 in patients with COVID-19. *Nat Med.* 2020 Apr 29;
- 516 4. Henderson LA, Canna SW, Schulert GS, Volpi S, Lee PY, Kernan KF, et al. On the
517 Alert for Cytokine Storm: Immunopathology in COVID-19. *Arthritis Rheumatol*
518 *Hoboken NJ.* 2020 Apr 15;
- 519 5. Chaussabel D. Assessment of immune status using blood transcriptomics and potential
520 implications for global health. *Semin Immunol.* 2015 Feb;27(1):58–66.
- 521 6. Zhou W, Altman RB. Data-driven human transcriptomic modules determined by
522 independent component analysis. *BMC Bioinformatics.* 2018 Sep 17;19(1):327.
- 523 7. Altman MC, Rinchai D, Baldwin N, Toufiq M, Whalen E, Garand M, et al.
524 Development and Characterization of a Fixed Repertoire of Blood Transcriptome
525 Modules Based on Co-expression Patterns Across Immunological States. *bioRxiv.* 2020
526 Apr 28;525709.
- 527 8. Ong EZ, Chan YFZ, Leong WY, Lee NMY, Kalimuddin S, Haja Mohideen SM, et al. A
528 Dynamic Immune Response Shapes COVID-19 Progression. *Cell Host Microbe.* 2020
529 Apr 30;
- 530 9. Xiong Y, Liu Y, Cao L, Wang D, Guo M, Jiang A, et al. Transcriptomic characteristics
531 of bronchoalveolar lavage fluid and peripheral blood mononuclear cells in COVID-19
532 patients. *Emerg Microbes Infect.* 2020 Jan 1;9(1):761–70.

- 533 10. Chaussabel D, Quinn C, Shen J, Patel P, Glaser C, Baldwin N, et al. A modular analysis
534 framework for blood genomics studies: application to systemic lupus erythematosus.
535 *Immunity*. 2008 Jul 18;29(1):150–64.
- 536 11. Chaussabel D, Baldwin N. Democratizing systems immunology with modular
537 transcriptional repertoire analyses. *Nat Rev Immunol*. 2014;14(4):271–80.
- 538 12. Gu Z, Eils R, Schlesner M. Complex heatmaps reveal patterns and correlations in
539 multidimensional genomic data. *Bioinforma Oxf Engl*. 2016 15;32(18):2847–9.
- 540 13. Hung IF-N, Lung K-C, Tso EY-K, Liu R, Chung TW-H, Chu M-Y, et al. Triple
541 combination of interferon beta-1b, lopinavir-ritonavir, and ribavirin in the treatment of
542 patients admitted to hospital with COVID-19: an open-label, randomised, phase 2 trial.
543 *Lancet Lond Engl*. 2020 May 8;
- 544 14. Malhotra S, Bustamante MF, Pérez-Miralles F, Rio J, Ruiz de Villa MC, Vegas E, et al.
545 Search for specific biomarkers of IFN β bioactivity in patients with multiple sclerosis.
546 *PloS One*. 2011;6(8):e23634.
- 547 15. Febbo PG, Mulligan MG, Slonina DA, Stegmaier K, Di Vizio D, Martinez PR, et al.
548 Literature Lab: a method of automated literature interrogation to infer biology from
549 microarray analysis. *BMC Genomics*. 2007 Dec 18;8:461.
- 550 16. Bhattacharya S, Dunn P, Thomas CG, Smith B, Schaefer H, Chen J, et al. ImmPort,
551 toward repurposing of open access immunological assay data for translational and
552 clinical research. *Sci Data*. 2018 27;5:180015.
- 553 17. Rinchai D, Altman MB, Konza O, Hässler S, Martina F, Toufiq M, et al. Identification
554 of erythroid cell positive blood transcriptome phenotypes associated with severe
555 respiratory syncytial virus infection. *bioRxiv*. 2020 May 10;527812.
- 556 18. Perng Y-C, Lenschow DJ. ISG15 in antiviral immunity and beyond. *Nat Rev Microbiol*.
557 2018;16(7):423–39.
- 558 19. Gutiérrez L, Caballero N, Fernández-Calleja L, Karkoulia E, Strouboulis J. Regulation
559 of GATA1 levels in erythropoiesis. *IUBMB Life*. 2020;72(1):89–105.
- 560 20. Elahi S. Neglected Cells: Immunomodulatory Roles of CD71+ Erythroid Cells. *Trends*
561 *Immunol*. 2019 Mar;40(3):181–5.
- 562 21. Obermoser G, Presnell S, Domico K, Xu H, Wang Y, Anguiano E, et al. Systems scale
563 interactive exploration reveals quantitative and qualitative differences in response to
564 influenza and pneumococcal vaccines. *Immunity*. 2013 Apr 18;38(4):831–44.
- 565 22. Roelands J, Garand M, Hinchcliff E, Ma Y, Shah P, Toufiq M, et al. Long-Chain Acyl-
566 CoA Synthetase 1 Role in Sepsis and Immunity: Perspectives From a Parallel Review of
567 Public Transcriptome Datasets and of the Literature. *Front Immunol*. 2019;10:2410.
- 568 23. Remy KE, Brakenridge SC, Francois B, Daix T, Deutschman CS, Monneret G, et al.
569 Immunotherapies for COVID-19: lessons learned from sepsis. *Lancet Respir Med*
570 [Internet]. 2020 Apr 28 [cited 2020 May 18];0(0). Available from:
571 [https://www.thelancet.com/journals/lanres/article/PIIS2213-2600\(20\)30217-4/abstract](https://www.thelancet.com/journals/lanres/article/PIIS2213-2600(20)30217-4/abstract)

- 572 24. Guo C, Li B, Ma H, Wang X, Cai P, Yu Q, et al. Tocilizumab treatment in severe
573 COVID-19 patients attenuates the inflammatory storm incited by monocyte centric
574 immune interactions revealed by single-cell analysis. *bioRxiv*. 2020 Apr
575 9;2020.04.08.029769.
- 576 25. Roumier M, Paule R, Groh M, Vallee A, Ackermann F. Interleukin-6 blockade for
577 severe COVID-19. *medRxiv*. 2020 Apr 22;2020.04.20.20061861.
- 578 26. Friedman S, Sanyal A, Goodman Z, Lefebvre E, Gottwald M, Fischer L, et al. Efficacy
579 and safety study of cenicriviroc for the treatment of non-alcoholic steatohepatitis in
580 adult subjects with liver fibrosis: CENTAUR Phase 2b study design. *Contemp Clin*
581 *Trials*. 2016 Mar 1;47:356–65.
- 582 27. Dogné J-M, Hanson J, de Leval X, Pratico D, Pace-Asciak CR, Drion P, et al. From the
583 design to the clinical application of thromboxane modulators. *Curr Pharm Des*.
584 2006;12(8):903–23.
- 585 28. Goicoechea M, García de Vinuesa S, Quiroga B, Verdalles U, Barraca D, Yuste C, et al.
586 Effects of pentoxifylline on inflammatory parameters in chronic kidney disease patients:
587 a randomized trial. *J Nephrol*. 2012 Dec;25(6):969–75.
- 588 29. Kahn-Kirby AH, Amagata A, Maeder CI, Mei JJ, Sideris S, Kosaka Y, et al. Targeting
589 ferroptosis: A novel therapeutic strategy for the treatment of mitochondrial disease-
590 related epilepsy. *PloS One*. 2019;14(3):e0214250.
- 591 30. Stockwell BR, Friedmann Angeli JP, Bayir H, Bush AI, Conrad M, Dixon SJ, et al.
592 Ferroptosis: A Regulated Cell Death Nexus Linking Metabolism, Redox Biology, and
593 Disease. *Cell*. 2017 Oct 5;171(2):273–85.
- 594 31. Wang C, Yuan W, Hu A, Lin J, Xia Z, Yang CF, et al. Dexmedetomidine alleviated
595 sepsis-induced myocardial ferroptosis and septic heart injury. *Mol Med Rep*. 2020
596 Jul;22(1):175–84.
- 597 32. Lang J, Yang N, Deng J, Liu K, Yang P, Zhang G, et al. Inhibition of SARS
598 pseudovirus cell entry by lactoferrin binding to heparan sulfate proteoglycans. *PloS*
599 *One*. 2011;6(8):e23710.
- 600 33. Shang J, Wan Y, Luo C, Ye G, Geng Q, Auerbach A, et al. Cell entry mechanisms of
601 SARS-CoV-2. *Proc Natl Acad Sci U S A*. 2020 May 6;
- 602 34. Li S-W, Wang C-Y, Jou Y-J, Huang S-H, Hsiao L-H, Wan L, et al. SARS Coronavirus
603 Papain-Like Protease Inhibits the TLR7 Signaling Pathway through Removing Lys63-
604 Linked Polyubiquitination of TRAF3 and TRAF6. *Int J Mol Sci*. 2016 May 5;17(5).
- 605 35. Frieman M, Yount B, Heise M, Kopecky-Bromberg SA, Palese P, Baric RS. Severe
606 acute respiratory syndrome coronavirus ORF6 antagonizes STAT1 function by
607 sequestering nuclear import factors on the rough endoplasmic reticulum/Golgi
608 membrane. *J Virol*. 2007 Sep;81(18):9812–24.
- 609 36. Li T, Wang P, Wang SC, Wang Y-F. Approaches Mediating Oxytocin Regulation of the
610 Immune System. *Front Immunol*. 2016;7:693.

- 611 37. Earnest JT, Hantak MP, Li K, McCray PB, Perlman S, Gallagher T. The tetraspanin
612 CD9 facilitates MERS-coronavirus entry by scaffolding host cell receptors and
613 proteases. *PLoS Pathog* [Internet]. 2017 Jul 31 [cited 2020 May 20];13(7). Available
614 from: <https://www.ncbi.nlm.nih.gov/pmc/articles/PMC5552337/>
- 615 38. Karulf M, Kelly A, Weinberg AD, Gold JA. OX40 ligand regulates inflammation and
616 mortality in the innate immune response to sepsis. *J Immunol Baltim Md 1950*. 2010
617 Oct 15;185(8):4856–62.
- 618 39. Tay MZ, Poh CM, Rénia L, MacAry PA, Ng LFP. The trinity of COVID-19: immunity,
619 inflammation and intervention. *Nat Rev Immunol*. 2020 Apr 28;1–12.
- 620 40. Azkur AK, Akdis M, Azkur D, Sokolowska M, van de Veen W, Brüggem M-C, et al.
621 Immune response to SARS-CoV-2 and mechanisms of immunopathological changes in
622 COVID-19. *Allergy*. 2020 May 12;
- 623 41. Giamarellos-Bourboulis EJ, Netea MG, Rovina N, Akinosoglou K, Antoniadou A,
624 Antonakos N, et al. Complex Immune Dysregulation in COVID-19 Patients with Severe
625 Respiratory Failure. *Cell Host Microbe*. 2020 Apr 17;
- 626 42. Sweeney TE, Perumal TM, Henao R, Nichols M, Howrylak JA, Choi AM, et al. A
627 community approach to mortality prediction in sepsis via gene expression analysis. *Nat*
628 *Commun*. 2018 15;9(1):694.
- 629 43. Yan Q, Li P, Ye X, Huang X, Mo X, Wang Q, et al. Longitudinal peripheral blood
630 transcriptional analysis of COVID-19 patients captures disease progression and reveals
631 potential biomarkers. *medRxiv*. 2020 May 8;2020.05.05.20091355.
- 632 44. Speake C, Whalen E, Gersuk VH, Chaussabel D, Odegard JM, Greenbaum CJ.
633 Longitudinal monitoring of gene expression in ultra-low-volume blood samples self-
634 collected at home. *Clin Exp Immunol*. 2017;188(2):226–33.
- 635 45. Rinchai D, Anguiano E, Nguyen P, Chaussabel D. Finger stick blood collection for gene
636 expression profiling and storage of tempus blood RNA tubes. *F1000Research*.
637 2016;5:1385.
- 638 46. Rinchai D, Konza O, Hassler S, Martina F, Mejias A, Ramilo O, et al. Characterizing
639 blood modular transcriptional repertoire perturbations in patients with RSV infection: a
640 hands-on workshop using public datasets as a source of training material. *bioRxiv*. 2019
641 Jan 22;527812.
- 642 47. Speake C, Presnell S, Domico K, Zeitner B, Bjork A, Anderson D, et al. An interactive
643 web application for the dissemination of human systems immunology data. *J Transl*
644 *Med*. 2015 Jun 19;13:196.
- 645 48. Linsley PS, Speake C, Whalen E, Chaussabel D. Copy number loss of the interferon
646 gene cluster in melanomas is linked to reduced T cell infiltrate and poor patient
647 prognosis. *PloS One*. 2014;9(10):e109760.
- 648 49. Bougarn S, Boughorbel S, Chaussabel D, Marr N. A curated transcriptome dataset
649 collection to investigate the blood transcriptional response to viral respiratory tract
650 infection and vaccination. *F1000Research*. 2019;8:284.

- 651 50. Parnell G, McLean A, Booth D, Huang S, Nalos M, Tang B. Aberrant cell cycle and
652 apoptotic changes characterise severe influenza A infection--a meta-analysis of genomic
653 signatures in circulating leukocytes. *PloS One*. 2011 Mar 8;6(3):e17186.
- 654 51. Ayllon-Benitez A, Bourqui R, Thébault P, Mougin F. GSA_n: an alternative to
655 enrichment analysis for annotating gene sets. *NAR Genomics Bioinforma* [Internet].
656 2020 Jun 1 [cited 2020 Apr 1];2(2). Available from:
657 <https://academic.oup.com/nargab/article/2/2/lqaa017/5805305>
- 658 52. Ambade A, Lowe P, Kodys K, Catalano D, Gyongyosi B, Cho Y, et al. Pharmacological
659 Inhibition of CCR2/5 Signaling Prevents and Reverses Alcohol-Induced Liver Damage,
660 Steatosis, and Inflammation in Mice. *Hepatology*. 2019;69(3):1105–21.
- 661 53. Winkler DG, Faia KL, DiNitto JP, Ali JA, White KF, Brophy EE, et al. PI3K- δ and
662 PI3K- γ inhibition by IPI-145 abrogates immune responses and suppresses activity in
663 autoimmune and inflammatory disease models. *Chem Biol*. 2013 Nov 21;20(11):1364–
664 74.
- 665 54. Wang S-M, Wang C-T. APOBEC3G cytidine deaminase association with coronavirus
666 nucleocapsid protein. *Virology*. 2009 May 25;388(1):112–20.
- 667 55. Milewska A, Kindler E, Vkovski P, Zeglen S, Ochman M, Thiel V, et al. APOBEC3-
668 mediated restriction of RNA virus replication. *Sci Rep*. 2018 13;8(1):5960.
- 669 56. de Lang A, Osterhaus ADME, Haagmans BL. Interferon-gamma and interleukin-4
670 downregulate expression of the SARS coronavirus receptor ACE2 in Vero E6 cells.
671 *Virology*. 2006 Sep 30;353(2):474–81.
- 672 57. Sisk JM, Frieman MB, Machamer CE. Coronavirus S protein-induced fusion is blocked
673 prior to hemifusion by Abl kinase inhibitors. *J Gen Virol*. 2018;99(5):619–30.
- 674 58. Song R, Lisovsky I, Lebouché B, Routy J-P, Bruneau J, Bernard NF. HIV protective
675 KIR3DL1/S1-HLA-B genotypes influence NK cell-mediated inhibition of HIV
676 replication in autologous CD4 targets. *PLoS Pathog*. 2014 Jan;10(1):e1003867.
- 677 59. Yeung M-L, Yao Y, Jia L, Chan JFW, Chan K-H, Cheung K-F, et al. MERS
678 coronavirus induces apoptosis in kidney and lung by upregulating Smad7 and FGF2.
679 *Nat Microbiol*. 2016 Feb 22;1:16004.
- 680 60. Li S-W, Wang C-Y, Jou Y-J, Yang T-C, Huang S-H, Wan L, et al. SARS coronavirus
681 papain-like protease induces Egr-1-dependent up-regulation of TGF- β 1 via ROS/p38
682 MAPK/STAT3 pathway. *Sci Rep*. 2016 13;6:25754.
- 683 61. Padhan K, Tanwar C, Hussain A, Hui PY, Lee MY, Cheung CY, et al. Severe acute
684 respiratory syndrome coronavirus Orf3a protein interacts with caveolin. *J Gen Virol*.
685 2007 Nov;88(Pt 11):3067–77.
- 686 62. Lindner HA, Lytvyn V, Qi H, Lachance P, Ziomek E, Ménard R. Selectivity in ISG15
687 and ubiquitin recognition by the SARS coronavirus papain-like protease. *Arch Biochem*
688 *Biophys*. 2007 Oct 1;466(1):8–14.

- 689 63. Riva L, Yuan S, Yin X, Martin-Sancho L, Matsunaga N, Burgstaller-Muehlbacher S, et
690 al. A Large-scale Drug Repositioning Survey for SARS-CoV-2 Antivirals. *bioRxiv*.
691 2020 Apr 17;2020.04.16.044016.
- 692 64. Liu M, Yang Y, Gu C, Yue Y, Wu KK, Wu J, et al. Spike protein of SARS-CoV
693 stimulates cyclooxygenase-2 expression via both calcium-dependent and calcium-
694 independent protein kinase C pathways. *FASEB J Off Publ Fed Am Soc Exp Biol*. 2007
695 May;21(7):1586–96.
- 696 65. Shi C-S, Nabar NR, Huang N-N, Kehrl JH. SARS-Coronavirus Open Reading Frame-8b
697 triggers intracellular stress pathways and activates NLRP3 inflammasomes. *Cell Death*
698 *Discov*. 2019;5:101.
- 699 66. Siu K-L, Yuen K-S, Castaño-Rodríguez C, Ye Z-W, Yeung M-L, Fung S-Y, et al.
700 Severe acute respiratory syndrome coronavirus ORF3a protein activates the NLRP3
701 inflammasome by promoting TRAF3-dependent ubiquitination of ASC. *FASEB J Off*
702 *Publ Fed Am Soc Exp Biol*. 2019;33(8):8865–77.
- 703 67. Qi F, Qian S, Zhang S, Zhang Z. Single cell RNA sequencing of 13 human tissues
704 identify cell types and receptors of human coronaviruses. *Biochem Biophys Res*
705 *Commun*. 2020 May 21;526(1):135–40.
- 706 68. Li D, Wu N, Yao H, Bader A, Brockmeyer NH, Altmeyer P. Association of RANTES
707 with the replication of severe acute respiratory syndrome coronavirus in THP-1 cells.
708 *Eur J Med Res*. 2005 Mar 29;10(3):117–20.
- 709 69. Follis KE, York J, Nunberg JH. Furin cleavage of the SARS coronavirus spike
710 glycoprotein enhances cell-cell fusion but does not affect virion entry. *Virology*. 2006
711 Jul 5;350(2):358–69.
- 712 70. Zhou Y, Vedantham P, Lu K, Agudelo J, Carrion R, Nunneley JW, et al. Protease
713 inhibitors targeting coronavirus and filovirus entry. *Antiviral Res*. 2015 Apr;116:76–84.

714

715

716 **FIGURE LEGENDS**

717

718 **Figure 1: Mapping Covid-19 blood transcriptome signatures at the module aggregate**

719 **level.** The columns on this heatmap represent samples (Xiong *et al.* & Ong *et al.*) or patient

720 cohorts (Altman *et al.*). Module aggregates (A1-A38) are arranged as rows. The colored

721 spots represent the proportion of transcripts comprising each transcriptional module

722 aggregate found to be differentially expressed compared to control samples. The cutoffs

723 vary from one study to another due to differences in the design and the profiling platforms

724 used. Thus, module aggregate response values range from 100% (all transcripts comprised
725 in the module aggregate increased) to -100% (all decreased). The Xiong *et al.* dataset
726 comprised one control and three Covid-19 patients and transcript abundance was measured
727 by RNA-seq. The Ong *et al.* dataset comprised three Covid-19 cases from whom samples
728 were collected serially, and nine uninfected controls (8). Transcript abundance was
729 measured using a 594 gene standard immune panel from Nanostring. Patterns are also
730 shown for cohorts comprised in the Altman *et al.* dataset (7). The colored labels (right)
731 indicate functional associations for some of the aggregates.

732

733 **Figure 2. Delineation of sets of Covid-19 relevant A31 modules. A. Transcript**
734 **abundance profiles of A31 modules in Covid-19 patients.** This heatmap represents the
735 abundance levels for transcripts forming modules belonging to aggregate A31 (rows), across
736 three Covid-19 patients (P1-P3) relative to one uninfected control subject (columns). The
737 data are expressed as the proportion of constitutive transcripts in each module being
738 significantly increased (red circles) or decreased (blue circles) relative to N1. **B. Transcript**
739 **abundance profiles of A31 modules in reference disease cohorts.** The top heatmap
740 represents the abundance levels for transcripts forming modules belonging to aggregate
741 A31 (rows), across 16 reference patient cohorts (columns). The bottom heatmaps represent
742 the changes in abundance across the individuals comprised in two relevant patient cohorts,
743 including pediatric patients with severe influenza or RSV infection and adult patients with
744 sepsis.

745

746 **Figure 3. Delineation of sets of Covid-19 relevant A28 modules. A. Transcript**
747 **abundance profiles of A28 modules in Covid-19 patients.** This heatmap shows the
748 abundance levels for transcripts forming modules belonging to aggregate A28 (rows), across
749 three Covid-19 patients (P1-P3) relative to one uninfected control subject (columns). The
750 data are expressed as the proportion of constitutive transcripts in each module being
751 significantly increased (red circles) or decreased (blue circles) relative to N1 **B. Transcript**

752 **abundance profiles of A28 modules in reference disease cohorts.** The top heatmap
753 shows the abundance levels for transcripts forming modules belonging to aggregate A28
754 (rows), across 16 reference patient cohorts (columns). The bottom heatmaps show changes
755 in abundance across individuals constituting the two relevant patient cohorts, including
756 pediatric patients with severe influenza or RSV infection and adult patients with sepsis.

757

758 **Figure 4 Changes in abundance of transcripts comprising aggregate A28 in response**
759 **to SARS-CoV-2 infection.** The heatmaps display the changes in transcript abundance in
760 three Covid-19 patients comprising the Xiong *et al.* RNA-seq transcriptome datasets. The
761 top heatmap summarizes the module-level values for the six modules forming aggregate
762 A28. The color code indicates membership to one of the three Covid-19 module sets that
763 were defined earlier. The bottom heatmap shows patterns of abundance for the same six
764 modules, but at the individual gene level. The line graphs on the right show changes in
765 abundance for three transcripts from the “therapeutic relevance panel” in three Covid-19
766 patients profiled by Ong *et al.* using a generic Nanostring immune set comprising 594
767 transcripts.

768

769

770 **Figure 5: High resolution annotation framework supporting the curation and**
771 **interpretation of Covid-19 module sets.** This series of screenshots shows the content of
772 the interactive presentations that have been established to provide curators with access to
773 detailed annotations regarding modules forming a given aggregate, its constitutive modules
774 and targets that have been selected for inclusion in transcript panels. Links to interactive
775 presentations and resources mentioned below are available in **Table 2. A. Module**
776 **aggregate-level information.** This section displays patterns of transcript abundance across
777 the modules forming a given aggregate, as well as the degree of association of this
778 aggregate with the severity of RSV disease. Plots used to populate this section were
779 generated using three web applications, including one that was developed in support of this

780 work that compiles the Covid-19 blood transcriptional data available to date. The other two
781 applications were developed as part of a previous study to generate plots for the reference
782 disease cohorts and RSV severity association plots (46). **B. Module-level information.**
783 This section includes, for a given module, reports from functional profiling tools as well as
784 patterns of transcript abundance across the genes forming the module. Drug targeting
785 profiles were added to provide another level of information. **C. Gene-centric information.**
786 The information includes curated pathways from the literature, articles and reports from
787 public resources. Gene-centric transcriptional profiles that are available via gene expression
788 browsing applications deployed by our group are also captured and used for context (GXB).
789 A synthesis of the information gathered by expert curation and potential relevance to SARS-
790 Cov-2 infection can also be captured and presented here.

791

792

793 **Supplementary Figure 1: Coverage of the pre-established 38 transcriptional module**
794 **aggregate repertoire by the Nanostring immunology panel 2.** The bar graphs show the
795 distribution of the 579 transcript constituting the standard Nanostring immunology panel
796 used by Ong *et al.* across the 38 module aggregates forming this repertoire. The Venn
797 diagram shows the degree of overlap between the Nanostring panel and the transcripts
798 forming this modular repertoire.

799

800 **Table 1:** List of Covid-19 relevant aggregates and module sets

801

Module Aggregate	Module Set	Modules	Functional annotations
A1	A1/S1	M14.42, M15.38, M12.6, M13.27,	T cells
	A1/S2	M14.23, M15.87, M14.5, M14.49, M12.1, M14.20	Gene transcription
	A1/S3	M12.8, M15.29, M14.58, M15.51, M14.64, M16.78, M14.75, M15.82, M14.80	B cells
A2	A2/S1	M13.21, M9.1	Cytotoxic lymphocytes
	A2/S2	M14.13, M14.72, M13.13, M13.14, M14.45, M13.10, M15.91	TBD
A4	A4/S1	M16.69, M16.72, M16.50, M16.77	Antigen presentation,
A5	A5/S1	M16.95, M16.36	B cells
	A5/S2	M16.57, M16.18, M16.65, M16.111, M16.99	B cells
A7	A7/S1	M15.61	Monocytes
A8	A8/S1	M16.30	Complement
	A8/S2	M16.106	TBD
A10	A10/S1	M15.102	Prostanoids
A26	A26/S1	M12.2	Monocytes
A27	A27/S1	M13.32, M12.15, M16.92, M15.110, M16.60	Antibody producing cells
A28	A28/S1	M15.127, M8.3	Interferon response
	A28/S2	M15.64	Interferon response
	A28/S3	M15.86, M10.1, M13.17	Interferon response
A31	A31/S1	M16.64	Platelet/Prostaglandin
	A31/S2	M15.58	Monocytes
A33	A33/S1	M15.104, M14.82, M14.24, M15.108	Cytokines/chemokines, Inflammation
	A33/S2	M14.19, M14.76, M14.50, M14.26, M16.101, M16.100, M16.80	Inflammation
A34	A34/S1	M14.59, M10.3, M16.109, M8.2	Platelets, Prostanoids
A35	A35/S1	M14.65, M14.28, M15.81, M16.79, M13.3, M14.7,	Monocytes, Neutrophils
	A35/S2	M15.26, M12.10, M13.22, M15.109, M15.78, M13.16,	Neutrophils, Inflammation
A36	A36/S1	M16.34, M16.82, M15.97, M14.51, M15.118, M16.88	Gene transcription
A37	A37/S1	M9.2, M14.53, M11.3, M12.11, M15.100 M15.74, M13.26, M13.30, M15.53,	Erythroid cells
A38	A38/S1	M10.4	Neutrophil activation
	A38/S2	M16.96, M12.9, M14.68	Erythroid cells

802 **Table 2:** Resources used for annotation and interpretation
803

Platform / Use	Name	Source	Notes	Link	Demo video	Ref.
Interactive presentations (Prezi) Exploration of aggregated annotations / curation / capture interpretation of functional relevance in the context of Covid-19 disease	Covid-19 Module Sets annotation framework	In house / open	See Figure 5 for details	A31: https://prezi.com/view/zYCSLyo0nvJTwfJkJqb/ A28: https://prezi.com/view/7lbgGwfiNffqQzvL14/)	Part 1: https://youtu.be/7sNE3e5W5g Part 2: https://youtu.be/l6wHrrmbet4 Part 3: https://youtu.be/iHnM7OHnw8	Present work
R Shiny Web Applications/ Exploration of module-level and gene-level blood transcriptome profiling data. Design and export of custom plots to populate the annotation framework.	Covid-19 app	In house / open	Provides access to two Covid-19 blood transcript profiling datasets. More will be added as they become available.	https://drinchai.shinyapps.io/COVID_19_project/	https://youtu.be/XhQZj9mm2ME	Present work
	Gen3 app	In house / open	Provides access to 16 reference patient cohorts datasets	https://drinchai.shinyapps.io/dc_gen3_module_analysis/#	https://youtu.be/y7xKJo5e4	Altman et al. (7)
	RSV app	In house / open	Provides access to six public RSV blood transcriptome datasets.	https://drinchai.shinyapps.io/RSV_Meta_Module_analysis/	https://youtu.be/htNSMr eM8es	Rinchai et al. (17)
Gene Expression Browser (GXB). Interactive browsing of expression profiles for individual transcripts. Themed curated dataset collections have been created.	GXB sepsis collection	In house / open	Makes 93 curated datasets relevant to sepsis	http://sepsis.gxbsidra.org/dm3/geneBrowser/list	https://youtu.be/D1rGYfVSAoM	Toufiq et al. (in preparation), and Speake et al. (47)
			A reference dataset presenting transcript abundance profiles across purified leukocyte populations	http://sepsis.gxbsidra.org/dm3/geneBrowser/show/4000098		Linsley et al. (48)
			Reference dataset presenting the response to <i>in vitro</i> blood stimulations	http://sepsis.gxbsidra.org/dm3/geneBrowser/show/4000152		Obermoser et al. (21)
	GXB Acute Respiratory Infection	In house / open	34 curated datasets relevant to acute respiratory infections	http://vri1.gxbsidra.org/dm3/geneBrowser/list	Bougarn et al. (49)	
			Reference dataset presenting changes in blood transcript abundance in patients with pneumonia	http://vri1.gxbsidra.org/dm3/miniURL/view/Mh	Parnell et al. (50)	
Gene Set Annotation tool.	GSAN	Third party / open		https://gsan.la-bri.fr/		Allion-Benitez et al. (51)
Pathway Analysis tool	Ingenuity Pathway	Third party / commercial	Pathway enrichment. Used for expert	https://digitalinsights.qiagen.		

	Analysis		curation of candidates.	com/products-overview/discoverly-insights-portfolio/analysis-and-visualization/qigen-ipa/		
Accumenta Biotech LiteratureLab Literature profiling and keyword enrichment tool	LitLab Gene Retriever	Collaboration with Third party / commercial	Retrieves genes from a collection of literature records provided by the user	https://www.accenta.com/generetriever		
Drug target identification	Open targets	Third party / open	Identifies drug targets among a list of gene candidates	https://www.targetvalidation.org/		
Retrieval of lists of immune-relevant genes	Immport	Third party / open	Provides access to curated gene lists	https://immport.org/shared/home		Bhattacharya et al. (16)

804
805
806
807
808

809
810
811
812

Table 3: Illustrative targeted panel – Immunology relevance focus

Module set	Module ID	NCBI Entrez ID	Symbol	Name	Module set functional annotation
A1/S1	M15.38	916	CD3E	CD3e molecule	T cells
A1/S2	M14.49	974	CD79B	CD79b molecule	Gene transcription
A1/S3	M14.80	3122	HLA-DRA	major histocompatibility complex, class II, DR alpha	B cells
A2/S1	M9.1	3002	GZMB	granzyme B	Cytotoxic lymphocytes
A2/S2	M13.13	4282	MIF	macrophage migration inhibitory factor	TBD
A4/S1	M16.77	3811	KIR3DL1	killer cell immunoglobulin like receptor, three Ig domains and long cytoplasmic tail 1	Antigen presentation
A5/S1	M16.95	972	CD74	CD74 molecule	B cells
A5/S2	M16.111	27242	TNFRSF21	TNF receptor superfamily member 21	B cells
A7/S1	M15.61	23166	STAB1	stabilin 1	Monocytes
A8/S1	M16.30	3600	IL15	interleukin 15	Complement
A8/S2	M16.106	57823	SLAMF7	SLAM family member 7	TBD
A10/S1	M15.102	246	ALOX15	arachidonate 15-lipoxygenase	Prostanoids
A26/S1	M12.2	942	CD86	CD86 molecule	Monocytes
A27/S1	M12.15	608	CD38	CD38 molecule	Cell Cycle
A28/S1	M8.3	9636	ISG15	ISG15 ubiquitin like modifier	Interferon response
A28/S2	M15.64	10475	TRIM38	tripartite motif containing 38	Interferon response
A28/S3	M10.1	115362	GBP5	guanylate binding protein 5	Interferon response
A31/S1	M16.64	1950	EGF	epidermal growth factor	Platelet/Prostaglandin
A31/S2	M15.58	2214	FCGR3A	Fc fragment of IgG receptor IIIa	Monocytes
A33/S1	M14.24	91	ACVR1B	activin A receptor type 1B	Cytokines/chemokines, Inflammation
A33/S2	M14.19	23765	IL17RA	interleukin 17 receptor A	Inflammation
A34/S1	M8.2	3674	ITGA2B	integrin subunit alpha 2b	Platelets, Prostanoids
A35/S1	M13.3	1241	LTB4R	leukotriene B4 receptor	Inflammation
A35/S2	M12.10	51311	TLR8	toll like receptor 8	Neutrophils, Inflammation
A36/S1	M16.34	2993	GYPA	glycophorin A (MNS blood group)	Gene transcription
A37/S1	M11.3	2623	GATA1	GATA binding protein 1	Erythroid cells
A38/S1	M10.4	4057	LTF	lactotransferrin	Neutrophil activation
A38/S2	M16.96	56729	RETN	resistin	Erythroid cells

813
814
815

816
817
818

Table 4: Illustrative targeted panel – Therapeutic relevance focus

Module set	Module ID	NCBI Entrez ID	Symbol	Name	Relevance	Notes
A1/S1	M15.38	916	CD3E	CD3e molecule	Immunological	Not suitable for targeting (adaptive immunity)
A1/S2	M14.49	974	CD79B	CD79b molecule	Immunological	Not suitable for targeting (adaptive immunity)
A1/S3	M14.80	3122	HLA-DRA	major histocompatibility complex, class II, DR alpha	Immunological	Not suitable for targeting (adaptive immunity)
A2/S1	M9.1	3002	GZMB	Granzyme B	Immunological	Not suitable for targeting (adaptive immunity)
A2/S2	M13.13	4282	MIF	Macrophage migration inhibitory factor	Immunological	Not suitable for targeting (adaptive immunity -presumed)
A4/S1	M16.77	3811	KIR3DL1	Killer cell immunoglobulin like receptor, three Ig domains and long cytoplasmic tail 1	Immunological	Not suitable for targeting (adaptive immunity)
A5/S1	M16.95	972	CD74	CD74 molecule	Immunological	Not suitable for targeting (adaptive immunity)
A5/S2	M16.111	27242	TNFRSF21	TNF receptor superfamily member 21	Immunological	Not suitable for targeting (adaptive immunity)
A7/S1	M15.61	23166	STAB1	stabilin 1	Immunological	No suitable candidates identified
A8/S1	M16.30	1728	NQO1	NAD(P)H quinone dehydrogenase 1	Therapeutic	Vatiquinone (EPI-743) has been found to inhibit ferroptosis (29), a process associated with tissue injury (30), including in sepsis (31).
A8/S2	M16.106	57823	SLAMF7	SLAM family member 7	Immunological	No suitable candidates identified
A10/S1	M15.102	246	ALOX15	Arachidonate 15-lipoxygenase	Immunological	No suitable candidates identified
A26/S1	M12.2	729230	CCR2	C-C motif chemokine receptor 2	Therapeutic	Anti-inflammatory properties have been attributed to the CCR2/CCR5 blocker Cenicriviroc (52)
A27/S1	M12.15	608	TNFRSF17	TNF receptor superfamily member 17	Immunological	Not suitable for targeting (adaptive immunity)
A28/S1	M8.3	4599	MX1	MX dynamin like GTPase 1	Therapeutic	Inducible by Interferon-beta treatment
A28/S2	M15.64	1230	CCR1	C-C motif chemokine receptor 1	Therapeutic	Inducible by Interferon-beta treatment
A28/S3	M10.1	3433	IFIT2	interferon induced protein with tetratricopeptide repeats 2	Therapeutic	Inducible by Interferon-beta treatment
A31/S1	M16.64	6915	TBXA2R	Thromboxane A2 receptor	Therapeutic	Thromboxane A2 synthase inhibitors have antiplatelet aggregation activities and anti-inflammatory activities (drugs include: Defibrotide / Seratrodast, Ozagrel)
A31/S2	M15.58	5743	PTGS2	Prostaglandin-endoperoxide	Therapeutic	PTGS2 encodes COX-2. Several specific inhibitors

				synthase 2		are available which possess anti-inflammatory properties (e.g. celecoxib, rofecoxib, valdecoxib).
A33/S1	M15.104	5151	PDE8A	Phosphodiesterase 8A	Therapeutic	PDE8A, is targeted by Pentoxifylline, a non-selective phosphodiesterase inhibitor that increases perfusion and may reduce risk of acute kidney injury and attenuates LPS-induced inflammation
A33/S2	M14.19	23765	IL17RA	Interleukin 17 receptor A	Therapeutic	Brodalumab may be beneficial in reducing the viral illness exacerbation. But current recommendation is discontinuation of use in COVID 19
A34/S1	M16.109	5742	PTGS1	Prostaglandin-endoperoxide synthase 1	Therapeutic	Encodes for Cox-1. COX inhibitors including Aspirin, Indomethacin, Naproxen have direct antiviral properties as well as anti-inflammatory and antithrombotic properties
A35/S1	M15.81	5293	PIK3CD	phosphatidylinositol-4,5-bisphosphate 3-kinase catalytic subunit delta	Therapeutic	PI3K-δ and PI3K-γ Inhibition by IPI-145 Abrogates Immune Responses and Suppresses Activity in Autoimmune and Inflammatory Disease Models (53)
A35/S2	M15.109	3570	IL6R	Interleukin 6 receptor	Therapeutic	IL6R is a target for the biologic drug Tocilizumab. Several studies have tested this antagonist in open label single arm trials in Covid-19 patients with the intent of blocking the cytokine storm associated with Covid-19 disease (15,16)
A36/S1	M16.34	2993	GYPA	glycophorin A (MNS blood group)	Immunological	Not suitable for targeting (erythropoiesis)
A37/S1	M11.3	2623	GATA1	GATA binding protein 1	Immunological	Not suitable for targeting (erythropoiesis)
A38/S1	M10.4	4057	LTF	Lactotransferrin	Immunological	No suitable candidates identified
A38/S2	M16.96	56729	RETN	Resistin	Immunological	Not suitable for targeting (erythropoiesis)

819
820
821
822

823 **Table 5:** Illustrative targeted panel – SARS biology relevance focus
824

Module set	Module ID	NCBI Entrez ID	Symbol	Name	Relevance	Notes
A1/S1	M15.38	916	CD3E	CD3e molecule	Immunological	
A1/S2	M12.1	60489	APOBEC3G	apolipoprotein B mRNA editing enzyme catalytic subunit 3G	CoV Biology	APOBEC3G associates with SARS viral structural proteins (54), with a possible role in restriction of RNA virus replication (55)
A1/S3	M14.64	51284	TLR7	toll like receptor 7	CoV Biology	TLR7 Signaling Pathway is inhibited by SARS Coronavirus Papain-Like Protease (34)
A2/S1	M13.21	3458	IFNG	interferon gamma	CoV Biology	Interferon-gamma and interleukin-4 Downregulate Expression of the SARS Coronavirus Receptor ACE2 (56)
A2/S2	M13.10	25	ABL1	ABL proto-oncogene 1, non-receptor tyrosine kinase	CoV Biology	Abl Kinase inhibitors block SARS-CoV fusion (57)
A4/S1	M16.77	3811	KIR3DL1	killer cell immunoglobulin like receptor, three Ig domains and long cytoplasmic tail 1	Immunological	The inhibitory KIR3DL1 is a strong ligand for HLA Bw4, C1 and C2 groups. High expression of this inhibitory KIR was associated with slower disease progress to AIDS and better HIV viral load control (58)
A5/S1	M16.65	4092	SMAD7	SMAD family member 7	CoV Biology	MERS Coronavirus Induces Apoptosis in Kidney and Lung by Upregulating Smad7 and FGF2 (59)
A5/S2	M16.111	27242	TNFRSF21	TNF receptor superfamily member 21	Immunological	
A7/S1	M15.61	1958	EGR1	early growth response 1	CoV Biology	SARS Coronavirus Papain-Like Protease Induces Egr-1-dependent Up-Regulation of TGF- β 1 (60)
A8/S1	M16.30	857	CAV1	caveolin 1	CoV Biology	Severe Acute Respiratory Syndrome Coronavirus Orf3a Protein Interacts with Caveolin (61)
A8/S2	M16.106	57823	SLAMF7	SLAM family member 7	Immunological	
A10/S1	M15.102	246	ALOX15	arachidonate 15-lipoxygenase	Immunological	
A26/S1	M12.2	942	CD86	CD86 molecule	Immunological	
A27/S1	M12.15	608	TNFRSF17	TNF receptor superfamily member 17	Immunological	
A28/S1	M8.3	9636	ISG15	ISG15 ubiquitin like modifier	CoV Biology	SARS-CoV PLpro exhibits ISG15 precursor processing activities (62)
A28/S2	M15.64	1230	CCR1	C-C motif chemokine receptor 1	CoV Biology	MLN-3897, a CCR1 antagonist inhibits replication of SARS-CoV-2 replication (63)
A28/S3	M10.1	6772	STAT1	signal transducer and activator of transcription 1	CoV Biology	SARS ORF6 Antagonizes STAT1 Function (35)
A31/S1	M16.64	1950	EGF	epidermal growth factor	Immunological	
A31/S2	M15.58	5743	PTGS2	prostaglandin-endoperoxide synthase 2	CoV Biology	Encodes COX2, which expression is stimulated by SARS Spike protein (64)
A33/S1	M14.24	114548	NLRP3	NLR family pyrin domain containing 3	CoV Biology	Multiple SARS-Coronavirus protein have been reported to activates

						NLRP3 inflammasomes (65,66)
A33/S2	M14.19	23765	IL17RA	interleukin 17 receptor A	Immunological	
A34/S1	M8.2	3674	ITGA2B	Integrin subunit alpha 2b	Immunological	
A35/S1	M13.3	1241	LTB4R	Leukotriene B4 receptor	Immunological	
A35/S2	M15.78	290	ANPEP	alanyl aminopeptidase, membrane	CoV Biology	A potential receptor for human CoVs (67)
A36/S1	M16.88	6352	CCL5	C-C motif chemokine ligand 5	CoV Biology	CCL5/RANTES is associated with the replication of SARS in THP-1 Cells (68)
A37/S1	M13.26	5045	FURIN	Furin, paired basic amino acid cleaving enzyme	CoV Biology	Furin cleavage of the SARS coronavirus spike glycoprotein enhances cell-cell fusion (69)
A38/S1	M10.4	4057	LTF	Lactotransferrin	CoV Biology	Lactotransferrin blocks the binding of the SARS-CoV spike protein to host cells, thus exerting an inhibitory function at the viral attachment stage (32)
A38/S2	M12.9	1508	CTSB	Cathepsin B	CoV Biology	Activation of SARS- and MERS-coronavirus is mediated cathepsin L (CTSL) and cathepsin B (CTSB) (70)

825
826
827
828
829
830

Table 6: List of housekeeping genes that may be suitable for blood transcript profiling applications

Housekeeping Genes	NCBI Entrez ID	Symbol	Name
Housekeeping Gene	1794	DOCK2	dedicator of cytokinesis 2
Housekeeping Gene	1915	EEF1A1	eukaryotic translation elongation factor 1 alpha 1
Housekeeping Gene	90268	FAM105B/ OTULIN	OTU deubiquitinase with linear linkage specificity
Housekeeping Gene	2512	FTL	ferritin light chain
Housekeeping Gene	103910	MYL12B/MRLC2	myosin light chain 12B
Housekeeping Gene	4637	MYL6	myosin light chain 6
Housekeeping Gene	6204	RPS10	ribosomal protein S10
Housekeeping Gene	6230	RPS25	ribosomal protein S25

831
832
833
834

835

836

837

838

839 **SUPPLEMENTAL INFORMATION**

840 Supplemental File 1: Delineation of Covid-19 relevant modules sets in all 17 aggregates

841 retained in the first step of the selection process.

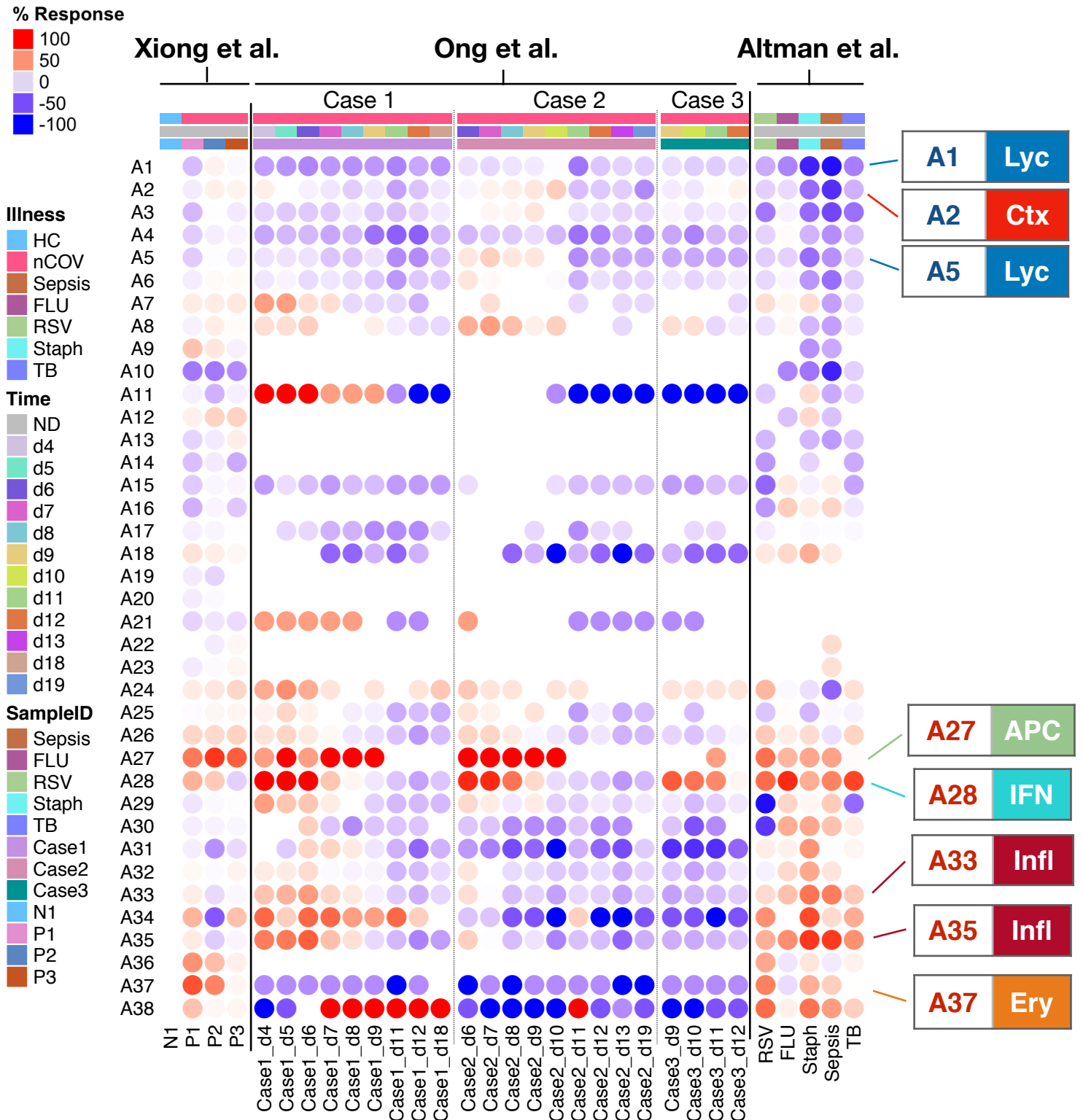
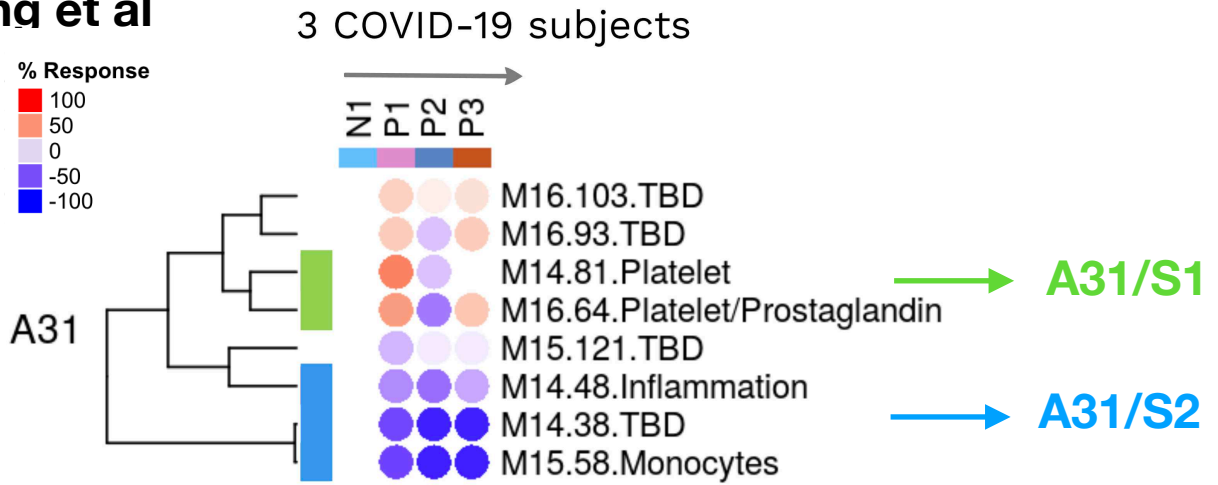


Figure 1

A. Xiong et al



B. Altman et al

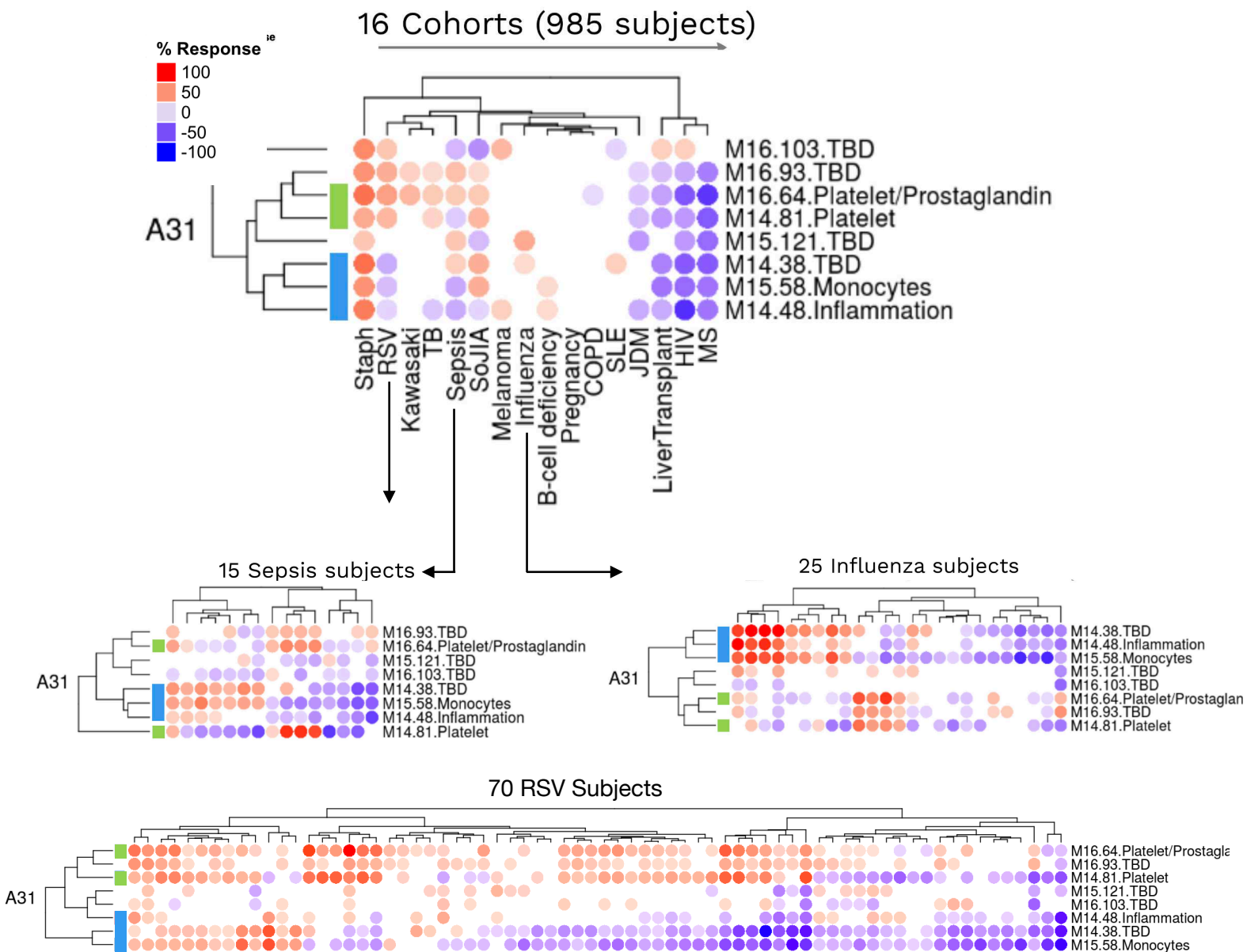
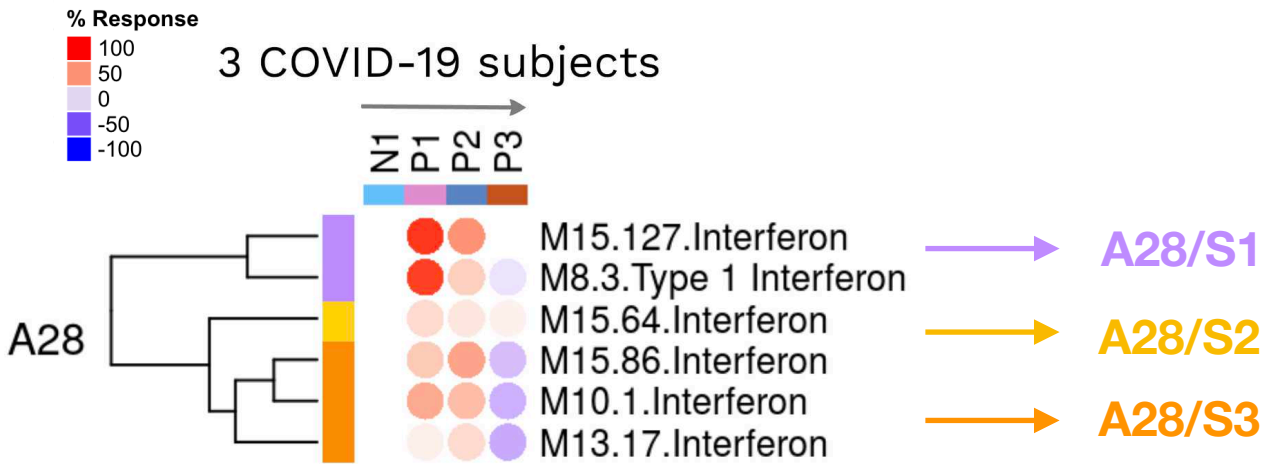


Figure 2

A. Xiong et al



B. Altman et al

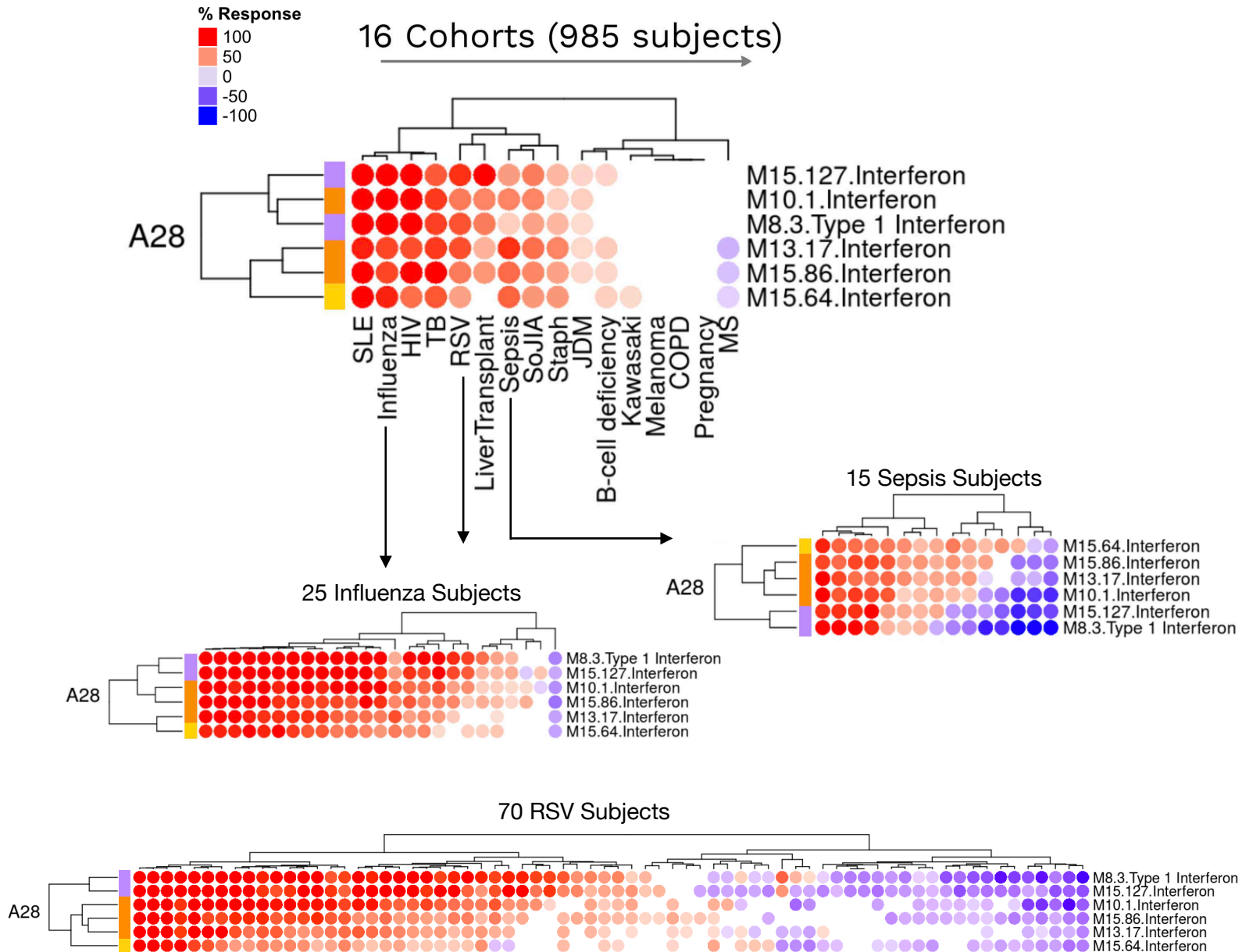
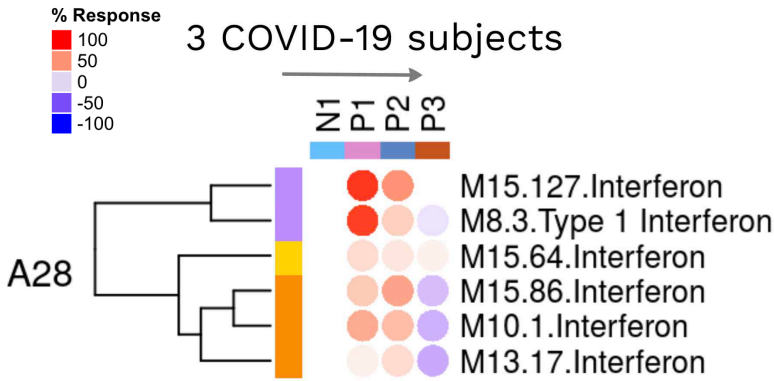


Figure 3

Xiong et al



A28/S1

A28/S2

A28/S3

Ong et al

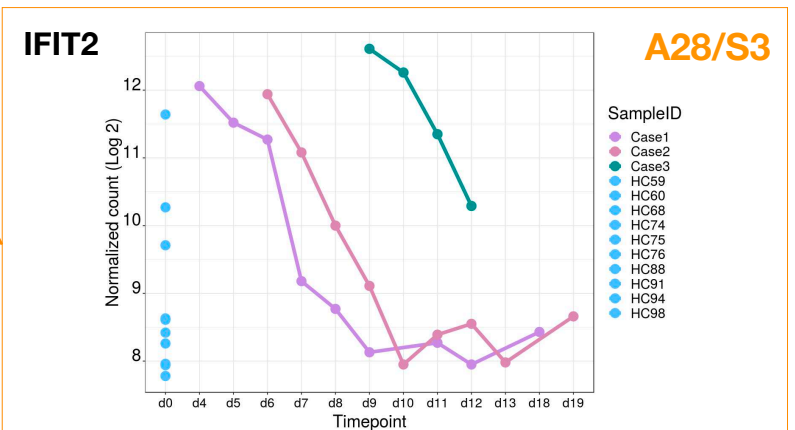
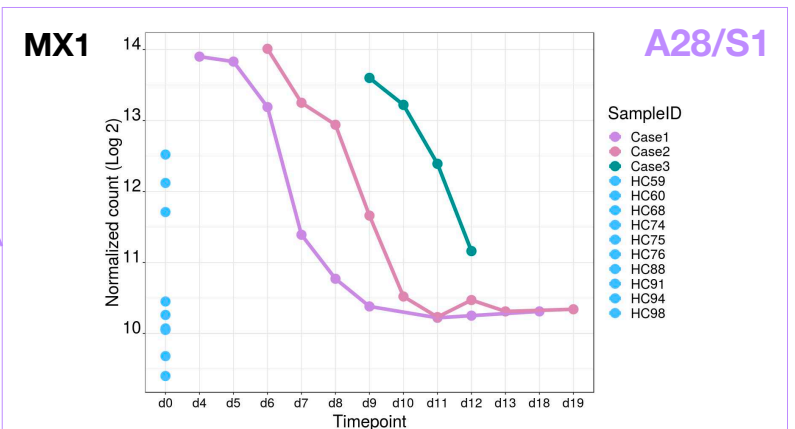
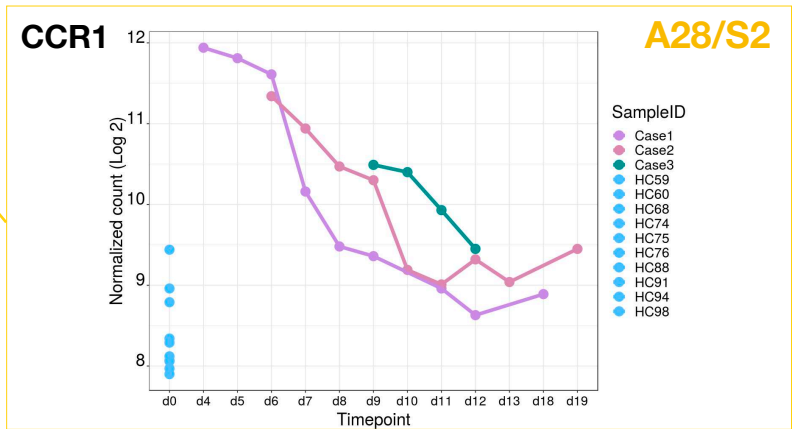
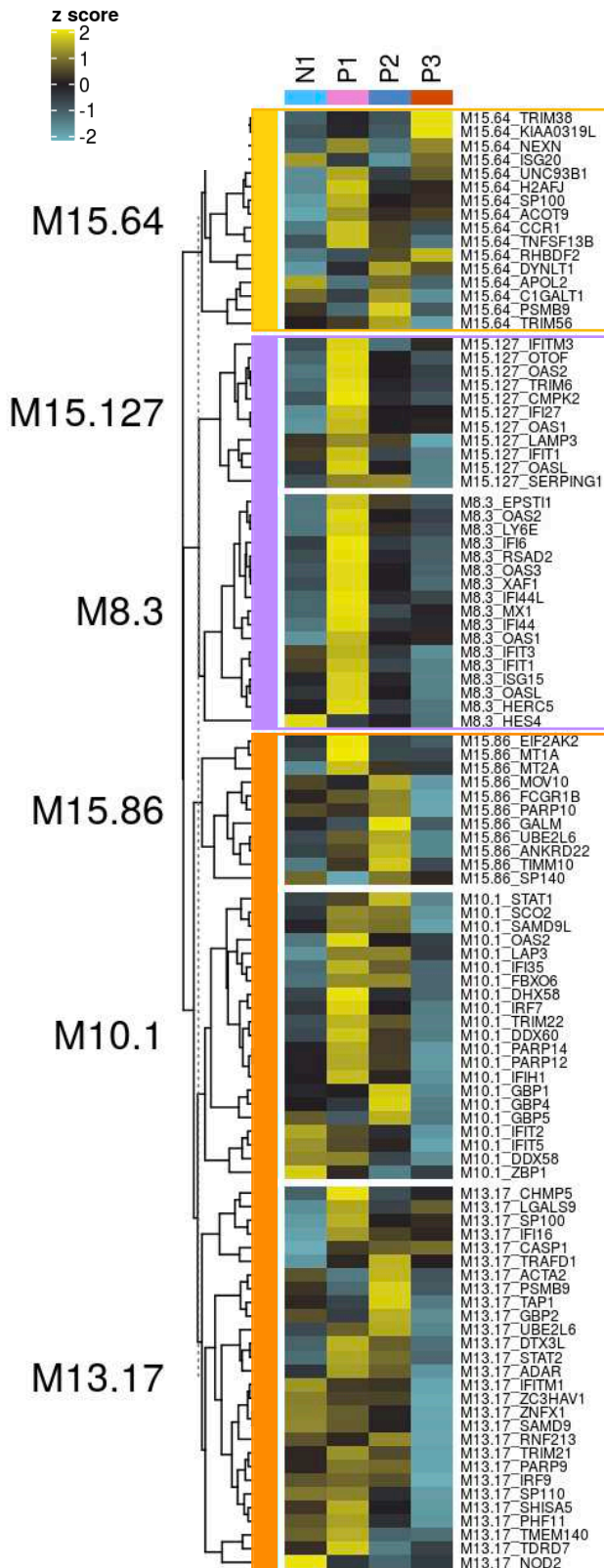
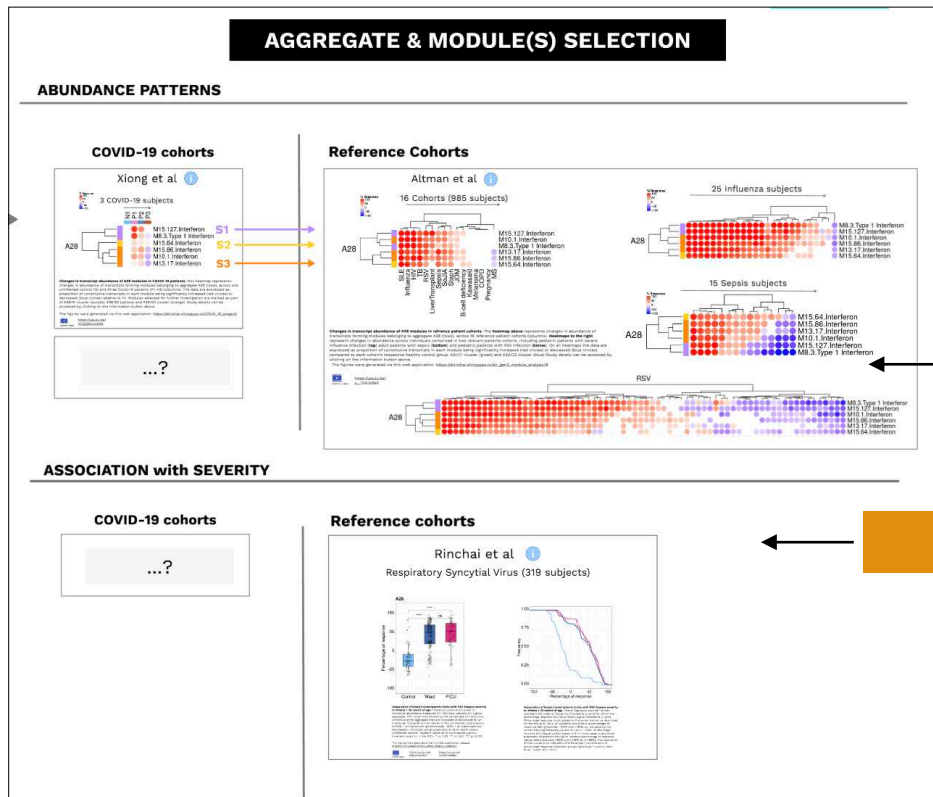
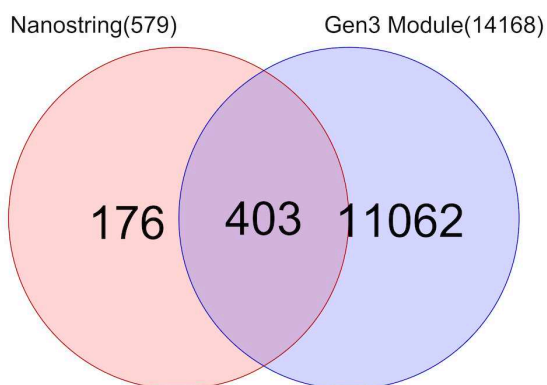
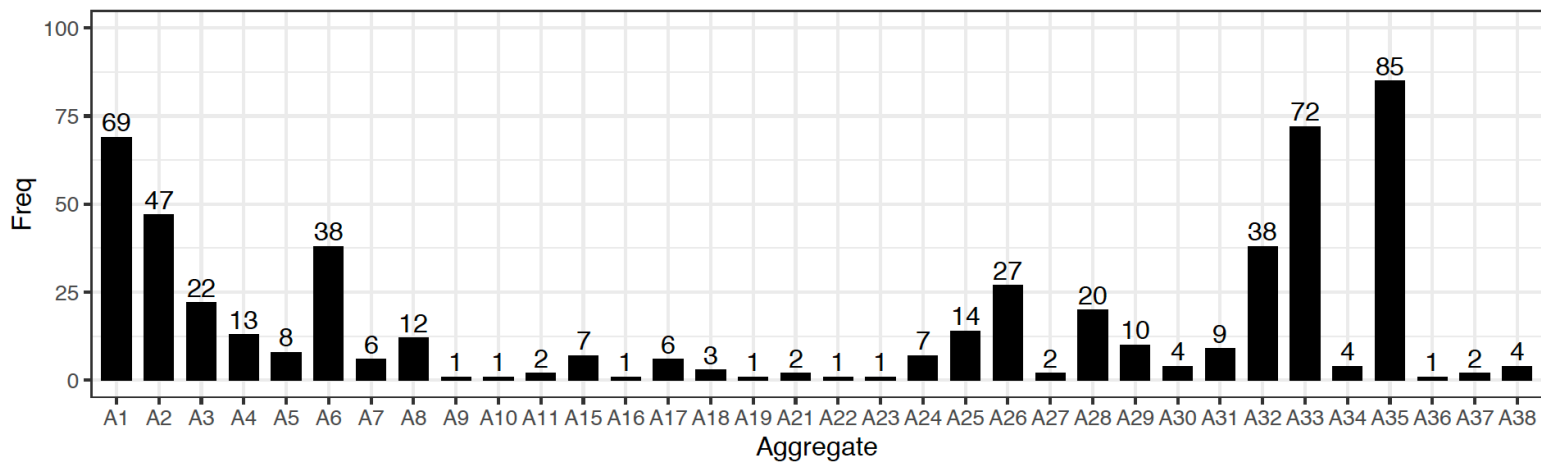


Figure 4

A.





Supplementary Files

This is a list of supplementary files associated with this preprint. Click to download.

- [2020May21CHMSupplementFileallCOVIDModulesets.pdf](#)